



Sensor fault detection and isolation: a game theoretic approach

Hamed Habibi, Ian Howard & Reza Habibi

To cite this article: Hamed Habibi, Ian Howard & Reza Habibi (2018) Sensor fault detection and isolation: a game theoretic approach, International Journal of Systems Science, 49:13, 2826-2846, DOI: [10.1080/00207721.2018.1526347](https://doi.org/10.1080/00207721.2018.1526347)

To link to this article: <https://doi.org/10.1080/00207721.2018.1526347>



Published online: 28 Sep 2018.



Submit your article to this journal [↗](#)



Article views: 128



View related articles [↗](#)



View Crossmark data [↗](#)



Sensor fault detection and isolation: a game theoretic approach

Hamed Habibi ^a, Ian Howard^a and Reza Habibi^b

^aFaculty of Science and Engineering, School of Civil and Mechanical Engineering, Curtin University, Perth, Australia; ^bIran Banking Institute, Central Bank of Iran, Tehran, Iran

ABSTRACT

This paper studies sensor fault detection using a game theoretic approach. Sensor fault detection is considered as change point analysis in the coefficients of a regression model. A new method for detecting faults, referred to as two-way fault detection, is introduced which defines a game between two players, i.e. the fault detectors. In this new strategic environment, assuming that the independent states of the regression model are known, the test statistics are derived and their finite sample distributions under the null hypothesis of no change are derived. These test statistics are useful for testing the fault existence, as well as, the pure and mixed Nash equilibriums are derived for at-most-one-change and epidemic change models. A differential game is also proposed and solved using the Pontryagin maximum principle. This solution is useful for studying the fault detection problem in unknown state cases. Kalman filter and linear matrix inequality methods are used in finding the Nash equilibrium for the case of unknown states. Illustrative examples are presented to show the existence of the Nash equilibriums. Also, the proposed fault detection scheme is numerically evaluated via its application on a practical system and its performance is compared with the cumulative sum method.

ARTICLE HISTORY

Received 12 October 2017
Accepted 16 September 2018

KEYWORDS

AMOC; differential game; epidemic model; Kalman filtering; LMI; Nash equilibrium; Pontryagin maximum principle; two-way fault detection

1. Introduction

From industrial safety systems to sustainable plants, fault detection and isolation (FDI) techniques play an essential role to detect and isolate faults in systems as early as possible and to generate the critical information which will be used to remove the fault effect from the overall system and keep the performance at the desirable level till the next prescheduled maintenance procedure (Ren, Ding, & Li, 2017; Song and Guo, 2017). In fact, implementing active fault tolerant control, in which FDI is an important step to prepare the fault information, reduces the shut-down periods and unplanned maintenance, also it can be used to prevent the component faults from degrading further into catastrophic failure and increases system reliability, especially for systems operating in harsh environments, e.g. offshore wind turbines (Habibi, Nohooji, & Howard, 2017b). It is also profitable to utilise the fault information obtained from FDI in manual maintenance approaches (Habibi, Howard, & Habibi, 2017a).

Generally, the aberration of system parameters from their nominal/expected values can be seen as faults at the system level view point (Isermann, 2006). Process, actuators and sensors form the main sources of faults which should be detected via the FDI scheme (Li, Wang, Han, & Wei, 2017). The residual-based FDI scheme is

the most utilised one to detect the faults. In this scheme, by comparing the outputs of redundant identical components, either hardware or software components, the residual signal can be generated which contains the possible fault information. The significant deviation of the residual signal from zero can be translated as fault occurrence (Habibi, Howard, & Habibi, 2017a). The evaluation of the residual to deduce the fault occurrence is very challenging especially for nonlinear systems with sensor noise, model uncertainty and immeasurable system disturbance (Ren et al., 2017). In fact, these issues may lead to deviation of residual signal levels from zero which, in turn, leads to false FDI (Li et al., 2017). Also, simple threshold checking, i.e. if the residual level crosses the threshold then the fault is detected, may lead to missed or non-detected faults which is very likely in the case of incipient/small faults which may cause severe system performance degradation or even instability (Blanke, Kinnaert, Lunze, Staroswiecki, & Schröder, 2006).

Sensor failure is one of the important sources of faults which may lead to system performance degradation, because it is most likely that the sensor output will be used in feedback control design which may cause system instability or even system break down (Gu & Yang, 2017; Habibi, Howard, & Habibi, 2017a).

Accordingly, detection of sensor faults is a significant aspect that must be considered, and various methods have been proposed for faster and more accurate FDI schemes. The least squares method is one of the best and well-developed methods to extract signal characteristics and probable fault information (Chen & Lu, 2013; Dalei & Mohanty, 2016; Hong & Dhupia, 2014; Yunlong & Peng, 2012). In Ahmadizadeh, Zarei, and Karimi (2014), Zarei and Shokri (2014), a nonlinear unknown input observer was designed for robust sensor FDI. Similarly, in Aouaouda, Chadli, Shi, and Karimi (2015), for uncertain and disturbed discrete-time nonlinear models, a robust observer approach for FDI was proposed. Also, in Habibi, Howard, and Habibi (2017a), Mehranbod, Soroush, and Panjapornpon (2005), the Bayesian framework was utilised to detect and identify sensor faults. On the other hand, utilising the concept of fuzziness, in Wu and Ho (2009), a fuzzy filter was designed for robust FDI of Ito stochastic systems. Two best observers, including Kalman or sliding mode concepts, for sensor robust FDI were studied in Ben Brahim, Dhahri, Ben Hmida, and Sellami (2017), Pourbabaee, Meskin, and Khorasani (2016), Zhang, Swain, and Nguang (2015).

The game theory, as a powerful technique in control engineering, has profited from many philosophical and theoretical concepts like Nash equilibrium (Chung & Speyer, 1998). The game theory concept is applicable in many fields, e.g. H_∞ control (Başar & Bernhard, 2008) and optimal control (Evans, 2005). In Chung and Speyer (1998), Mutuel and Speyer (2000), the trade-off between FDI and disturbance attenuation has led to a game theoretic FDI filter. In Bresolin and Capiluppi (2013), the game theory concept was used to design a FDI scheme for a hybrid system which mixed continuous and discrete time dynamics. A discrete time FDI filter for a multiple fault case using the game theory concept was designed in Murray and Speyer (2014). In Elhadeif and Grira (2018), the fault diagnosis in distributed and parallel systems was studied using the game theory.

In this paper, the fault model is considered as a change in coefficient of the regression model, as the underlying framework for sensor FDI, which can capture a wide variety of sensor fault types. Indeed, the change point analysis of the coefficient of the regression model is studied for sensor FDI. So, the change point analysis and FDI are used interchangeably (Habibi, Howard, & Habibi, 2017a). Consider the sensor measurement as a regression model as,

$$y_t = \beta_t x_t + \varepsilon_t, t = 1, 2, \dots, n, \quad (1)$$

where y_t is sensor output, β_t is sensor coefficient, and ε_t is independent and identically distributed zero mean random variables with common variance $\sigma_\varepsilon^2 < \infty$. It is

assumed that the x_t 's are unknown state variables coming from a stochastic (deterministic) state equation as,

$$x_t = h(x_{t-1}, u_t) + e_t \quad (2)$$

for some functions h , where, u_t 's are control variables, for example, $u_t = Kx_t$ which is a state feedback control with control gain K . Here, e_t 's are random error terms independent of ε_t 's. In the deterministic cases, e_t 's are zero. As a special case, when h is a linear function, then $x_t = \alpha x_{t-1} + \gamma u_t + e_t$, where α and γ are real numbers (Habibi, Howard, & Habibi, 2017a). The null hypothesis H_0 states that there is no change in β_t for $t = 1, 2, \dots, n$, while the at-most-one-change (AMOC) alternative hypothesis H_1 implies that, there is a change at an unknown time $t^* = [n\tau^*]$, for $0 \leq \tau^* \leq 1$. $[\chi]$ represents the integer part of variable χ . Accordingly, H_1 is formulated as,

$$H_1 : \beta_t = \begin{cases} b_1, & t \leq t^*, \\ b_2, & t \geq t^* + 1, \end{cases} \quad (3)$$

where b_1 and b_2 are unknown sensor coefficients before and after the change moment t^* , respectively, and $b_1 \neq b_2$. The magnitude of change is $\varphi = b_2 - b_1$. An alternative choice for H_1 is the epidemic change model (Ning, Pailden, & Gupta, 2012) which is represented as,

$$H_1 : \beta_t = \begin{cases} b_1, & t \leq t_1^*, \\ b_2, & t_1^* + 1 \leq t \leq t_2^*, \\ b_1, & t_2^* + 1 \leq t \leq n. \end{cases} \quad (4)$$

Again, let $t_i^* = [n\tau_i^*]$, $i = 1, 2$, such that $0 < \tau_1^* < \tau_2^* < 1$. Accordingly, it is aimed to detect changes in β_t . It is noteworthy that in most practical dynamic systems, in the fault free case $\beta_t = 1$. Indeed, it is aimed to measure identically the given state. So, at the fault moment, after which $\beta_t \neq 1$, the sensor output is obviously not equal to the state. Accordingly, the fault model (3) or (4) can be translated as a multiplicative fault scenario. Also, the other types of faults including biased or fixed sensor output can be considered in this framework. For example, $\beta_t = 1 + (c - \varepsilon_t)/x_t$ and $\beta_t = (c - \varepsilon_t)/x_t$ represent the biased and fixed measurement in this framework, respectively, where c is a constant number. Accordingly, a family of sensor fault types can be modelled as multiplicative faults for which the proposed FDI scheme is applicable, which is captured via this framework.

In this paper the two-way FDI approach is proposed to resolve the problem of weak performance of conventional one-way FDI approaches. Also, the proposed approach induces a game theoretic framework for change point analysis. It should be noted that two-way and one-way

FDI approaches are accurately defined in Section 2. The differences and advantages of the two-way FDI approach compared to one-way method can be outlined as follows in five categories.

(a) Game theoretic arguments

(1) Game theory has different useful concepts such as equilibriums (Gibbons, 1992). Two-player FDI makes a game theoretic framework to use all useful game theory concepts in FDI. For example, although, in the current paper, the Nash equilibrium is used, however, the widely used method IEWDS (Iterated Elimination of Weakly Dominated Strategy) can be applied, in future researches. Also, some other famous framework in game theory such as different kinds of adoptions, repetitions, learning is applicable so the players can cover their mistakes in a cooperative framework. Different types of games like incomplete information (in simultaneously or sequentially form) are extendable. These are not applicable in one-way FDI framework.

(2) The game theory has applications in many fields of control engineering such as H_∞ control. Two-way FDI adds some different useful concepts such as games based on bias reduction, player test statistic, quasi-Bayesian, their equilibriums (mixed and pure), in AMOC and epidemic, their limiting behaviour, the use of LMI technique, as well as the important topic of differential games (known-unknown states), in the current paper.

(b) Data analysis arguments

The proposed method here can also be used as a data mining technique (it belongs to the diagnosis-supervisory category of data mining techniques). So it is expected to have some good properties which are listed as below.

- (3) Results seem to be more insensitive to outliers, missing values, and small shift problems, because two players may choose different detection methods that improve their estimation accuracy.
- (4) Since two estimators are derived by two players, the ultimate change point estimation is a function of two estimators, for example their means. Thus, the variance of the final estimator is smaller than the variance of both estimators.
- (5) Since the data sequence is checked for the existence of change points, it seems that the possibility of spurious change points being identified is decreased.

(6) The model is applicable for the use of multiple change point analysis. Indeed, as soon as a player detects a change point, other change points are detected sequentially by both players.

(7) In the epidemic change point detection, the use of only a small length of the epidemic period is very problematic. If one player misses and passes the period without identifying the change points, the other player may compensate for the first one's mistake.

(c) Speed of detection and performance arguments

(8) In the AMOC setting, the two-way FDI approach detects the change point faster than the one-way method. Indeed, it seeks for a change from both directions of the data series, and as soon as each player detects a change, the game is over.

(9) When the change point is close to the start or end of the data sequence, the performance of one-way FDI methods is often weak (Bai, 1994; Sen & Srivastava, 1975). In contrast, the performance of the two-way method is independent of the location of the change.

(d) Industrial arguments

(10) The application of two-way FDI is significant when it is used for periodic maintenance procedures, especially for industrial systems with large amounts of data, e.g. SCADA data in wind turbine farms (Yang, Court, & Jiang, 2013). In fact, using this method, without losing any critical information, the data exploitation time can be reduced significantly by analysing the data from both the beginning and the end of the data series (Hameed, Hong, Cho, Ahn, & Song, 2009; Qiu et al., 2012).

(e) Similarity to other detection methods

(11) Inherently, change point analysis methods use some search techniques for finding breaks and shifts in the parameters of statistical or mathematical models. There are many methods to increase the speed of the search and reduce the computational complexities. One of the famous methods is binary splitting with its advantages (Ho, 1998). Two-way FDI is a special type of binary splitting which has some of the good properties of the sampling splitting method such as the rate of convergence of the search induces to two-way FDI.

The main contribution of the current paper compared to the available literatures is that the sensor FDI problem is defined as a game theoretic problem utilising the two-way FDI approach. The existence of the Nash

equilibrium is then surveyed in various cases with different criteria, e.g. via minimising the bias of the player estimation of the sensor coefficient, before and after the fault moment, or by using the least squares method, the quasi-Bayesian method, and corresponding player test statistics (Habibi, Sadooghi-Alvandi, & Nematollahi, 2005). The differential game is proposed based on the above-mentioned test statistics and solved for known and unknown state cases. In the former case, the maximum principle is applied to solve the differential game, while in the latter one, it is solved using two approaches, including linear matrix inequality (LMI) and the maximum principle, when the states are estimated by the Kalman filter. The finite sample null distribution of the test statistic is derived when state x_t is a sorted sample of the uniform distribution, or a linear combination of x_{t-1} and u_t , or when it is estimated via the Kalman filtering approach. Also, using the best response function approach, the Nash equilibrium is derived. The Nash equilibrium is derived when both players decide to minimise the bias of their estimations of the parameter before and after the fault moment. It should be noted that, according to the best knowledge of the authors, there has been no attempt at studying the two-way sensor FDI, before this paper.

The rest of the paper is organised as follows. In Section 2, the game definition of two-way FDI is proposed. Then, using the best response function, by minimising the bias of sensor coefficient estimations before and after the fault moment, made by each player (detector), the two-way game framework is studied. Since each player wants to test the null hypothesis of the no change H_0 , individually, the test statistics are proposed. The asymptotic null distributions of test statistics are also presented. Finally, the two-way FDI game framework is constructed using the mentioned test statistics. In Section 3, the game theoretic FDI is presented for the known states case. The two-way FDI is studied for the AMOC and epidemic change models. The pure Nash equilibrium in three different perspectives and Petkov's (2013) mixed strategies are derived. A differential game is constructed based on these mentioned test statistics. In Section 4, the game theoretic two-way FDI is studied for the unknown states case. First, the LMI approach is proposed. Then, the Kalman filter is also proposed to estimate the unknown states and also for solving the differential game. Illustrative examples including finite sample distributions of test statistics, players best response functions, sensor bias, sensor fixed output, epidemic faults, and rolling analysis are studied in Section 5. Also, a practical example, i.e. integrated servo mechanism system, is considered to evaluate the superiority of the proposed FDI scheme. The conclusions are given in Section 6.

2. Game definition and test statistics

In this section the two-way game theoretic FDI framework is constructed based on the given criteria and corresponding test statistics are derived.

2.1. Game definition: two-Way FDI

The conventional FDI methods seek a change in β_t starting at y_1 and ending at y_n , sequentially, using online or offline disciplines, which is called the one-way FDI, in this paper. Under the AMOC alternative hypothesis H_1 and an offline discipline, the FDI problem is similar to a game between two players that aim to estimate the change point as well as to estimate b_1, b_2 . In this paper, a new concept of FDI, called two-way FDI, is proposed which allows the use of the game theoretic methods in FDI. Consider two players (detectors). The player 1 moves from y_1 to y_n and the player 2, in a reverse direction, from y_n to y_1 . Under H_0 , both players are greedy and rational because they want to use more observations in estimating b_1, b_2 . This is the game theoretic FDI under H_0 .

To describe the game theoretic aspects under H_1 , consider the special case of the AMOC model at which $x_t = 1$, for all $t \geq 1$. Hence, the estimations of b_1 and b_2 , made by players 1 and 2 are given as $\hat{b}_{1i} = (1/\hat{t}_i) \sum_{j=1}^{\hat{t}_i} y_j$ and $\hat{b}_{2i} = (1/(n - \hat{t}_i)) \sum_{j=1}^{n-\hat{t}_i} y_j$, $i = 1, 2$, respectively, where players 1 and 2 estimate t^* by \hat{t}_1 and $n - \hat{t}_2$, respectively. Each player is trying to minimise its own estimation bias. Given \hat{t}_1, \hat{t}_2 , the biases of these estimators are

$$\begin{aligned} bias_{1i} &= \begin{cases} 0, & \hat{t}_i \leq t^*, \\ \varphi \left(1 - \frac{t^*}{\hat{t}_i}\right), & \hat{t}_i \geq t^* + 1, \end{cases} \text{ and} \\ bias_{2i} &= \begin{cases} -\varphi \left(\frac{t^* - \hat{t}_i}{n - \hat{t}_i}\right), & \hat{t}_i \leq t^*, \\ 0, & \hat{t}_i \geq t^* + 1, \end{cases} \end{aligned} \quad (5)$$

where, notation $bias_{1i}$ stands for bias of \hat{b}_{1i} . Suppose that both players compare their estimations of b_1 , given by $(1/\hat{t}_1) \sum_{i=1}^{\hat{t}_1} y_i$ and $(1/\hat{t}_2) \sum_{i=1}^{\hat{t}_2} y_i$, respectively. Let $\delta_k = \hat{t}_k - t^*$, $k = 1, 2$. Table 1 gives the proportions of biases over φ that is the coordinates $(bias_{11}/\varphi, bias_{12}/\varphi)$ as a function of δ_1 and δ_2 . Cells marked by * are the pure Nash equilibrium for this game.

Indeed, when $\max(\hat{t}_1, \hat{t}_2) \leq t^*$, the Nash equilibrium occurs. Considering the biases for estimation of b_2 , the Nash equilibrium occurs at $\min(\hat{t}_1, \hat{t}_2) \leq t^*$. Combining both Nash equilibrium conditions, it is concluded that $\hat{t}_1 = \hat{t}_2 = t^*$. For another example, suppose that player

Table 1. Values of $(bias_{11}, bias_{12})/\varphi$.

Bias	$\delta_2 \leq 0$	$\delta_2 > 0$
$\delta_1 \leq 0$	$(0,0)^*$	$(0, \frac{\delta_2}{\delta_2 + t^*})$
$\delta_1 > 0$	$(\frac{\delta_1}{\delta_1 + t^*}, 0)$	$(\frac{\delta_1}{\delta_1 + t^*}, \frac{\delta_2}{\delta_2 + t^*})$

Table 2. Values of $(bias_{11}, bias_{22})/\varphi$.

Bias	$\delta_2 \leq 0$	$\delta_2 > 0$
$\delta_1 \leq 0$	$(0, \frac{\delta_2}{n - t^* - \delta_2})$	$(0,0)^*$
$\delta_1 > 0$	$(\frac{\delta_1}{\delta_1 + t^*}, \frac{\delta_2}{n - t^* - \delta_2})$	$(\frac{\delta_1}{\delta_1 + t^*}, 0)$

1 estimates b_1 and player 2 estimates b_2 . Then, Table 2 gives the values of $(bias_{11}/\varphi, bias_{22}/\varphi)$. The equilibrium occurs when the player 1 chooses $\hat{t}_1 \leq t^*$ and the player 2 considers the $\hat{t}_2 \geq t^* + 1$.

Although, in the previous simple game, each player played his game, individually. However, this simple game can be modified to be a corporative/competitive game as follows. In the AMOC model, suppose that players 1 and 2 estimate t^* as \hat{t}_1 and $n - \hat{t}_2$, respectively. The ultimate estimation of \hat{t} is a function of \hat{t}_1 and \hat{t}_2 . For example, if both players cooperate, then, $\hat{t} = 0.5(\hat{t}_1 + \hat{t}_2)$. In a competitive two-way FDI game, it is assumed that as soon as one player finds a change, that player wins, and the game is finished. Hence, $\hat{t} = \min(\hat{t}_1, \hat{t}_2)$. This competition is similar to Cournot's oligopoly, which is frequently used in economics and finance (Gibbons, 1992). The $\hat{\beta}_t$ and $\hat{\beta}_t^*$ are estimations of regression coefficients before and after the change, respectively. Sometimes, both players agree with the same location of change. For example, in a sequential format of the game, both of them use the same change detector procedure. In these cases, a test statistic for change detection is needed. The above-mentioned example was a simple case of two-way FDI. The other cases are considered in Section 3.

2.2. Players test statistics

In this section test statistics are given, such that, each player can detect the change point individually. Also, it should be noted that, besides the bias minimisation (see Section 2.1), game theoretic two-way FDI is constructed based on the given test statistics.

First, assume that states x_t 's are known and the AMOC model is considered. The unknown states case is studied in Section 4. The epidemic change problem is investigated in Section 3.3. When both players agree to test the existence of change at the same time t , ($t \leq n - 1$) the least square estimates of parameters (regression coefficients) before and after the change is given by

$$\hat{\beta}_t = \frac{\sum_{i=1}^t x_i y_i}{\sum_{i=1}^t x_i^2}, \hat{\beta}_t^* = \frac{\sum_{i=t+1}^n x_i y_i}{\sum_{i=t+1}^n x_i^2}. \quad (6)$$

Let $s_t = \sum_{i=1}^t x_i^2$ and $\lambda_t = \frac{s_t}{s_n}$, $t = 1, 2, \dots, n$, and suppose that

$$d_t = \hat{\beta}_t - \hat{\beta}_t^*, \quad (7)$$

where

$$\hat{\beta}_t = \lambda_t \hat{\beta}_{t-1} + (1 - \lambda_t) \left(\frac{y_t}{x_t} \right). \quad (8)$$

When the H_0 is correct, i.e. there is no change, then d_t oscillates around zero for each of the t 's and if for some t^* the $|d_{t^*}|$ is too large, it indicates that there is a change at t^* . This fact motivates one to use the following suitable test statistic

$$\max_{2 \leq t \leq n-1} |d_t|, \quad (9)$$

as a change detector. To standardise d_t , it is easily can be seen that

$$\text{var}(d_t) = \frac{\sigma_\varepsilon^2}{s_n \lambda_t (1 - \lambda_t)}. \quad (10)$$

Therefore, the standardised d_t is proportional to $\sqrt{\lambda_t (1 - \lambda_t)} |d_t|$. Hence, the test statistic is given by,

$$\max_{2 \leq t \leq n-1} \sqrt{\lambda_t (1 - \lambda_t)} |d_t|. \quad (11)$$

Using some algebraic manipulations, it can be seen that $\hat{\beta}_t^* = ((\hat{\beta}_n - \lambda_t \hat{\beta}_t)/(1 - \lambda_t))$ and $d_t = ((\hat{\beta}_n - \hat{\beta}_t)/(1 - \lambda_t))$. Thus, the test statistic (11) is modified as,

$$\max_{2 \leq t \leq n-1} |u_t^n|, \quad (12)$$

where, $u_t^n = \sqrt{\lambda_t (1 - \lambda_t)}^{-1} (\hat{\beta}_t - \hat{\beta}_n)$. The estimation of change point t^* is then given by,

$$\text{argmax}_{2 \leq t \leq n-1} |u_t^n|. \quad (13)$$

Assuming the change point t^* is bounded from the start or end of the data sequence, i.e. $t^* \in I = [a, b]$ where $a = [n\theta]$ and $b = [n(1 - \theta)]$ for some positive small number θ , then, each player test statistic is given by,

$$T_{n,\theta}^1 = \max_{t \in I} |u_t^n|. \quad (14)$$

The u_t^n plot is close to zero when there is no change in β_t . When there is a sudden change in β_t 's, the $|u_t^n|$ plot shows a pattern going out from some specified boundaries with high probability (see Section 5.1). The mentioned boundaries are obtained using the asymptotic or finite sample distributions of test statistics (see Sections 2.3 and 5.1 part (a)).

To illustrate that $|u_t^n|$ takes its maximum at the actual change point, a simple example is given in the AMOC setting, as $n = 1000$ and $t^* = 500$, $b_1 = 2$, $b_2 = 3$, $\sigma_\varepsilon = 0.5$ and x_t 's are the sorted sequence of n independent and uniformly distributed variables on $(0, 1)$. Then, the

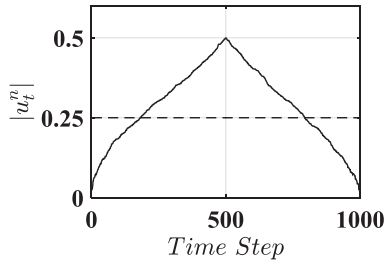


Figure 1. Time series plot $|u_t^n|$, uniform states.

resulting plot of $|u_t^n|$ is shown in Figure 1. It is obvious that the maximum point is at the change point and crosses the boundary 0.25. This boundary is calculated with Monte Carlo simulations with 1000 repetitions, and the empirical 95% quantile is considered as the boundary.

To apply this test procedure in the epidemic change model, it is necessary to find the first change and then apply the test procedure for observations after the first change to find the next change time point. An alternative method is to apply the two-way method based on the game theory approach which is described in Section 3.3.

When the x_t and β_t are vectors (in bolded notations) of size $p \geq 2$, the regression equation is $y_t = \mathbf{x}_t' \beta_t + \varepsilon_t$. The $\hat{\beta}_t$ is given by $\left(\sum_{i=1}^t \mathbf{x}_i' \mathbf{x}_i \right)^{-1} \sum_{i=1}^t \mathbf{x}_i' y_i$. Then, the test statistic is given by $\max_{t \in I} (\beta_t - \hat{\beta}_t^*)' \Lambda^{-1} (\beta_t - \hat{\beta}_t^*)$, where $\Lambda = \left(\sum_{i=1}^t \mathbf{x}_i' \mathbf{x}_i \right)^{-1} + \left(\sum_{i=t+1}^n \mathbf{x}_i' \mathbf{x}_i \right)^{-1}$. It is easy to see that for the case of $p = 1$, the above equation reduces to the $T_{n,\theta}^1$ and in the current paper, this case is enough for the proposed analysis.

Hereafter, the two-way FDI is constructed using test statistics. To this end, notice that, if each player wants to detect the change individually, independently, and they use $T_{n,\theta}^1$ in the offline discipline, then both estimate the change point as $\hat{t}_1 = \hat{t}_2$. However, if player 1 assumes that player 2 believes that the location of change is s , then the test statistic $T_{n,\theta}^1$ is given as the maximum value of $|u_{\min(t,s)}^n|$ over $t \in I$ given that s is kept fixed, i.e. $T_{n,\theta}^1 = \max_{t \in I} |u_{\min(t,s)}^n|$. The best response of player 1 (player 2), when player 2 (player 1) believes that the change is fixed at s (t), is given by $B_1(s) = \hat{t}_s = \arg \max_t |u_{\min(t,s)}^n|$ (or $B_2(t) = \hat{s}_t = \arg \max_s |u_{\min(t,s)}^n|$), where $B_1(s)$ ($B_2(t)$) is the best response of player 1 (player 2) when player 2 (player 1) believes that the change point is s (t). To illustrate that Nash equilibrium occurs at the actual change point, consider the time series plots of \hat{t}_s and \hat{s}_t , as given in Figure 2, for a simple example as follows. $n = 100$, $t^* = 20$, $b_1 = 1$, $b_2 = 5$, $\sigma_\varepsilon = 0.1$ and x_t 's come from $x_t = \alpha x_{t-1} + \gamma u_t + e_t$, and $u_t = Kx_t$, with $\alpha = 0.1$, $\gamma = 0.5$

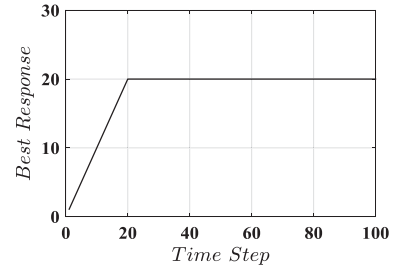


Figure 2. Time series plot of both \hat{t}_s and \hat{s}_t .

and $K = 0.2$. As it is obvious that a Nash equilibrium occurs at $t = s = 20$. As it is seen, $s = t = 20$ is the first τ at which $B_1(B_2(\tau)) = \tau$ and $B_2(B_1(\tau)) = \tau$ occurs as well as where utilities (payoffs) are maximised. Thus, a stable Nash equilibrium occurs at $t = s = 20$ (Gibbons, 1992). It should be noted that this scheme will be also investigated carefully in Section 5.2 with payoff function $u_{\min 0.5(t+s)}^n$.

As follows, theoretical arguments of the simulated results shown in Figure 2 are given. Notice that the test statistic of the player 1 is given by,

$$T_{n,\theta}^1 = \max_{t \in I} |u_{\min(t,s)}^n| = \max(\max_{t < s} |u_t^n|, |u_s^n|), \quad (15)$$

where s is the player 1's belief about the player 2's belief of change location. Then the change time point estimation is given by,

$$\hat{t}_s = \arg \max_t \{ \max(\max_{t < s} |u_t^n|, |u_s^n|) \}. \quad (16)$$

Also, the test statistic of the player 2 is,

$$T_{n,\theta}^2 = \max(\max_{s < t} |u_s^n|, |u_t^n|). \quad (17)$$

For both players the $u_{\min(t,s)}^n$ is very close to its expectation (for similar arguments, see Bai, 1994), and since its expectation is maximised at t^* then

$$\begin{aligned} \min(\hat{t}_s, s) &= t^*, \\ \min(\hat{s}_t, t) &= t^*. \end{aligned} \quad (18)$$

Thus, it is concluded that the Nash equilibrium is $s = t = t^*$ which shows that both players select the actual change point, correctly. A natural question is about the best combination of \hat{t}_1, \hat{t}_2 to find the ultimate estimation of \hat{t} . To answer this question, when both players use the criterion $|u_{0.5(t+s)}^n|$, again it is seen that

$$\begin{aligned} \hat{t}_s + s &= 2t^*, \\ \hat{s}_t + t &= 2t^*. \end{aligned} \quad (19)$$

A solution in this case is $s = t = t^*$. Again, both players select the actual change point.

Here, an alternative formulation of the test statistic and Nash equilibrium are presented. Following (Habibi et al., 2005; Kander and Zacks, 1966) the quasi-Bayesian method test statistic is given by

$$T_{n,\theta}^2 = \int_{\theta}^{1-\theta} \pi_s |u_{[ns]}^n| ds, \quad (20)$$

for some weighting function π_s . The above test statistic may be considered as a weighted average of u_t^n . Indeed, the integral functional is used in $T_{n,\theta}^2$ instead of maximum functional which used in $T_{n,\theta}^1$. The large values of the test statistic reject the null hypothesis H_0 . Thus, the null hypothesis of $T_{n,\theta}^2$ is needed to find the threshold c such that $T_{n,\theta}^2 > c$ rejects the null hypothesis H_0 . This method for change point detection in a general class of distributions has been applied in Habibi et al. (2005). Again, using criterion $u_{\min(t,s)}^n$ in $T_{n,\theta}^2$, it is seen that the test statistic of the player 1 is given by

$$\int_{\theta}^s \pi_t |u_{[nt]}^n| dt + |u_{[ns]}^n| \int_s^{1-\theta} \pi_t dt, \quad (21)$$

whereas the test statistic for the player 2 is

$$\int_{\theta}^t \pi_s |u_{[ns]}^n| ds + |u_{[nt]}^n| \int_t^{1-\theta} \pi_s ds. \quad (22)$$

If $u_{[nt]}^n$ and $u_{[ns]}^n$ are replaced by $u_{\min(t,s)}^n$ in (21) and (22), via considering the best response functions of both players, which maximise (21) and (22), it is easy to see that again the Nash equilibrium occurs at t^* .

2.3. Asymptotic null distributions

To make statistical inference about the existence of the change, as well as to find the boundaries mentioned in the previous Section, the asymptotic (limiting) null distributions of $T_{n,\theta}^i$, $i = 1, 2$ are needed. First, notice that under the null hypothesis H_0 , $\beta_t = \beta$ for $t = 1, 2, \dots, n$. Thus, $|\hat{\beta}_t - \hat{\beta}_n| = |\hat{\beta}_t - \beta - (\hat{\beta}_n - \beta)|$. That is, the null distribution of $T_{n,\theta}^i$ doesn't depend on β . So, it is assumed that $\beta = 0$. Also, notice that, based on the x_t 's being either deterministic or a stochastic sequence of numbers, the asymptotic null distributions differs. For example, in the x_t deterministic case, assuming, for each u , then

$$n^{-1} \sum_{i=1}^{[nu]} x_i^2 \rightarrow g(u), \quad (23)$$

then Proposition 2.1 gives the null limiting distribution of $T_{n,\theta}^1$. Let $H(u) = W(g(u)) - \frac{g(u)}{g(1)} W(g(1))$ and $G(u) = \{g(u)(1 - g(u))\}^{-0.5} H(g(u))$, where W is the standard Brownian motion on $[0, 1]$.

Proposition 2.1: Under H_0 , the limiting null distribution of $T_{n,\theta}^1$ is given as follows:

$$n^{-\frac{3}{2}} \sigma^{-1} T_{n,\theta}^1 \rightarrow^d \max_{u \in [\theta, 1-\theta]} G(u). \quad (24)$$

Notation \rightarrow^d stands for the convergence in the distribution.

Proof: Using the Donsker theorem (see, Billingsley, 2013), it is seen that $n^{-1/2} \sigma^{-1} \sum_{i=1}^{[nu]} x_i \varepsilon_i \rightsquigarrow W(g(u))$. Here, the weak convergence \rightsquigarrow occurs on the space $D[0, 1]$ on the Skorokhod topology. The $D[0, 1]$ is space of all functions that have limits to the left at each $t \in (0, 1]$ and are right-continuous functions. The Skorokhod topology is an alternative version of uniform topology (Billingsley, 2013). Also, notice that, $\frac{\sigma^{-1}}{n\sqrt{n}} |\hat{\beta}_{[nu]} - \hat{\beta}_n| = \frac{s_{[nu]}}{n} \left(\frac{\sigma^{-1}}{\sqrt{n}} \left| \sum_{i=1}^{[nu]} x_i \varepsilon_i - \frac{s_{[nu]}}{s_n} \sum_{i=1}^n x_i \varepsilon_i \right| \right) \rightsquigarrow g(u) |H(u)|$.

Hence, $n^{-\frac{3}{2}} \sigma^{-1} T_{n,\theta}^1 \rightarrow^d \max_{u \in [\theta, 1-\theta]} G(u)$. This completes the proof. ■

Corollary 2.1: (a)–(c) are true.

- (a) If $g(u) = u$, then process $H(u)$ is a standard Brownian bridge of $W(u)$ on $[0, 1]$.
- (b) In case of (a) and under H_0 , assuming $\left| \frac{\alpha}{1-\gamma K} \right| < 1$, then $T_{n,\theta}^1$ converges in distribution to the maximum of the Bessel process $\frac{W(u)-uW(1)}{\sqrt{u(1-u)}}$ (see Bai, 1994).
- (c) If $x_t = \alpha x_{t-1} + \gamma u_t + e_t$, with the feedback control variable $u_t = Kx_t$, which is a frequently used state equation in control engineering, again the deterministic results are true.

Proof: The proof of part (a) is straightforward and then omitted. For part (b), notice that, $x_t = \frac{\alpha}{1-\gamma K} x_{t-1} + \frac{1}{\alpha} e_t$, and this completes the proof part (b). The statistical properties of the Bessel process have been studied in Revuz and Yor (1999). The proof of part (c) is also straightforward. Here, using a Monte Carlo simulation, the quantiles of a Bessel process is simulated and consequently the boundaries mentioned in the previous section are derived. ■

The following proposition gives the limiting distribution of $T_{n,\theta}^1$, when condition $\left| \frac{\alpha}{1-\gamma K} \right| < 1$ is violated which is necessary for Proposition 2.1. To this end, suppose that $\alpha = 1 - \gamma K$ and W^* and W are two independent standard Brownian motions. Let $G^*(u) = \frac{X(u) - \frac{\Delta u}{\Delta_1} X(1)}{\sqrt{\Delta_u(1-\Delta_u)}}$ with $X(u) = \int_0^u W^*(s) dW(s)$ and $\Delta_u = \frac{\int_0^u W^{*2}(s) ds}{\int_0^1 W^{*2}(s) ds}$.

Proposition 2.2: Under the null hypothesis H_0 , and if $\alpha = 1 - \gamma K$, then

$$n^{-\frac{3}{2}}\sigma^{-1}T_{n,\theta}^1 \rightarrow^d \max_{u \in [\theta, 1-\theta]} G^*(u)/\alpha. \quad (25)$$

Proof: As $\alpha = 1 - \gamma K$, then sequence x_t 's have unit root and they are random walk, indeed, $x_i = \sum_{j=1}^i \frac{e_j}{\alpha}$. Assuming $\beta_i = \beta = 0$, then $\hat{\beta}_{[nu]} = \sum_{i=1}^{[nu]} x_i \varepsilon_i / \sum_{i=1}^{[nu]} x_i^2$ which converges weakly (as a stochastic process) to $(1/\alpha) \int_0^u W^*(s) dW(s) / \int_0^u W^{*2}(s) ds$. Thus, $n^{-\frac{3}{2}}\sigma^{-1}T_{n,\theta}^1 \rightarrow^d \max_{u \in [\theta, 1-\theta]} G^*(u)/\alpha$. This completes the proof. ■

Proposition 2.3: Under H_0 , then

$$n^{-\frac{3}{2}}\sigma^{-1}T_{n,\theta}^2 \rightarrow \int_{\theta}^{1-\theta} \pi_s \frac{|B(s)|}{\sqrt{s(1-s)}} ds. \quad (26)$$

Proof: The continuous mapping theorem (Billingsley, 2013) and convergence of $n^{-1/2}\sigma^{-1} \sum_{i=1}^{[nu]} x_i \varepsilon_i$ completes the proof. The Monte Carlo method may be applied to find the quantiles of $\int_{\varepsilon}^{1-\varepsilon} \pi_s \frac{|B(s)|}{\sqrt{s(1-s)}} ds$. ■

3. Two-way FDI: known states

In the previous section, the two-way FDI was constructed via test statistics of change point analysis. In this Section, it is assumed that states x_t 's are known. This assumption leads to finding the pure and mixture Nash equilibriums, appropriately. Also, it makes a framework to study the differential games and more complicated structures such as epidemic faults. The results can be extended to the unknown state cases which are studied in Section 4.

Assume that x_t 's are known. Without loss of generality, assume that $x_t = 1$, for all $t \geq 1$. To elaborate the reason, suppose that $x_t \neq 1$ for some t 's. The states of the following scaled regression model are one

$$\frac{y_t}{x_t} = \beta_t + \frac{\varepsilon_t}{x_t}, t = 1, 2, \dots, n \quad (27)$$

An interesting point is that the variance of variable ε_t/x_t is σ^2/x_t^2 which causes a heteroskedasticity property in the regression model (27). The weighted mean of $\frac{y_t}{x_t}$ (using $x_t^2 / \sum_{i=1}^n x_i^2$ as generalised least square weights) is exactly the $\hat{\beta}_t$. This fact shows that inferences based on both models (27) and (1) are equivalent. Hence, originally, assume that $x_t = 1$, for all $t \geq 1$, that is,

$$y_t = \beta_t + \varepsilon_t, t = 1, \dots, n. \quad (28)$$

In model (28), β_t is the mean of y_t . Therefore, the cumulative sum (CUMSUM) approach can be applied

for FDI. Using this new approach, as follows, the two-way pure and mixed Nash equilibriums are derived in the AMOC case. The differential games are studied and two-way FDI is studied for epidemic hypothesis.

3.1. Pure equilibrium

Here, for the AMOC case, the pure Nash equilibrium is studied in three different perspectives (a)-(c), as follows. First, notice that the i -th player ($i = 1, 2$), estimates the change $\tau_i \in (0, 1)$ (instead of $t_i = 1, 2, \dots, n-1$) by optimising the objective (utility) functions $u_i, i = 1, 2$ where,

$$\begin{aligned} u_1(\tau_1) &= \frac{1}{n} \sum_{i=1}^{[n\tau_1]} (y_i - \bar{y}), u_2(\tau_2) \\ &= \frac{1}{n} \sum_{i=1}^{n-[n\tau_2]} (y_{n-i+1} - \bar{y}). \end{aligned} \quad (29)$$

Suppose that player 1 estimates b_1 by $\bar{y}_{[n\tau_1]} = (1/[n\tau_1]) \sum_{i=1}^{[n\tau_1]} y_i$ and player 2 estimates b_2 by $\bar{y}_{[n\tau_2]}^* = (1/(n - [n\tau_1])) \sum_{i=1}^{n-[n\tau_2]} y_i$. Without loss of generality, assume that $\varphi \geq 0$. To test $H_0 : b_1 = b_2$, the test statistic is $\bar{y}_{[n\tau_1]} - \bar{y}_{[n\tau_2]}^*$. Similar to arguments in Section 2.1, it is seen that to reduce the biases of estimations of $\bar{y}_{[n\tau_1]}$ and $\bar{y}_{[n\tau_2]}^*$ as well as the bias of the test statistic $\bar{y}_{[n\tau_1]} - \bar{y}_{[n\tau_2]}^*$, it is enough to let $\tau_1 = \tau_2 = \tau^*$. Thus, the Nash equilibrium occurs at the actual change point τ^* .

(a) Similar to Section 2.2, suppose that the ultimate estimation of the change is $\tau = \min(\tau_1, \tau_2)$. Then, the best response of the i -th ($i = 1, 2$) player is given by

$$\begin{aligned} B_1(\tau_2) &= \operatorname{argmax}_{0 \leq \tau_1 \leq 1} |u_1(\tau)|, \\ B_2(\tau_1) &= \operatorname{argmax}_{0 \leq \tau_2 \leq 1} |u_2(\tau)|. \end{aligned} \quad (30)$$

One can see that u_1 and u_2 are very close to their means (Bai, 1994). Therefore,

$$u_1(\tau) \approx E(u_1(\tau)) = \begin{cases} -\varphi(1 - \tau^*)\tau, & \tau \leq \tau^*, \\ -\varphi\tau^*(1 - \tau), & \tau > \tau^*, \end{cases} \quad (31)$$

and $u_2(\tau) = -u_1(\tau)$. Also, notice that

$$u_1(\tau) = u_1(\min(\tau_1, \tau_2)) = \begin{cases} u_1(\tau_1), & \tau_1 \leq \tau_2, \\ u_1(\tau_2), & \tau_1 > \tau_2. \end{cases} \quad (32)$$

Here, $B_1(\tau_2)$ and $B_2(\tau_1)$ are found as follows. If $\tau_1 \leq \tau_2$ and $\tau_2 \leq \tau^*$, then $B_1(\tau_2) = \tau_2$. If $\tau_1 \leq \tau_2$ and $\tau_2 > \tau^*$, then $B_1(\tau_2) = \tau^*$. Therefore, when $\tau_1 \leq \tau_2$,

then $B_1(\tau_2) = \min(\tau_2, \tau^*)$. If $\tau_1 > \tau_2$, then $B_1(\tau_2) = [\tau_2, 1]$. In the current case, if $\tau_2 \leq \tau^*$, again $B_1(\tau_2) = \min(\tau_2, \tau^*)$. Hence, consider the case of $\tau_1 > \tau_2$ and $\tau_2 > \tau^*$, again, it is easy to see that $u_1(\tau_2) < u_1(\tau^*)$, thus, for all cases,

$$B_1(\tau_2) = \min(\tau_2, \tau^*). \quad (33)$$

Also, it can be seen that $B_1(\tau) = B_2(\tau)$. Therefore, a Nash equilibrium occurs at τ^* .

- (a) (c) Again, assume that the ultimate estimation of the change is the minimum of change estimations of player 1 and player 2. Also, a version of rationality (additional to the regular rationality assumption the usually exists in game theoretic problems) is assumed for both players. Suppose that if players 1 and 2 understand that player 1's estimate of change is closer to the actual change than the change estimation of player 2, then they use u_2 , instead of u_1 , and vice versa. Then, following (Petkov, 2013), it is seen that this game doesn't have pure equilibrium.

The following proposition summarises the above discussion.

Proposition 3.1: *The actual change point τ^* is the pure Nash equilibrium of the two-way game under perspectives (a) and (b). Under (c), the pure Nash equilibrium does not exist.*

3.2. Mixed equilibrium

Consider the part (c) of Section 3.1. Since, the pure Nash equilibrium doesn't exist, it is interested to find the mixed Nash equilibrium. To this end, assume that both players randomise according to a distribution function F . Let the ultimate change point be $\min(\tau_1, \tau_2)$, where τ_1, τ_2 are player 1 and player 2 estimates of change point τ^* . Similar to part (c) of the previous Section, players 1 and 2 are rational. Then, following (Petkov, 2013), the expected payoff of player 1 (pay_1) is

$$\begin{aligned} pay_1 &= \int_0^1 u(\tau) dF(\tau_2) \\ &= \int_0^{\tau_1} u(\tau_2) dF(\tau_2) + \int_{\tau_1}^1 u(\tau_1) dF(\tau_2) \\ &= \int_0^{\tau_1} u_2(\tau_2) dF(\tau_2) + \int_{\tau_1}^1 u_1(\tau_1) dF(\tau_2) \\ &= \int_0^{\tau_1} u_2(\tau_2) dF(\tau_2) + (1 - F(\tau_1)) u_1(\tau_1) \end{aligned} \quad (34)$$

The mixed strategy is to choose F such that $\frac{\partial pay_1}{\partial \tau_1} = 0$, see (Gibbons, 1992). In this way, player 1 is indifferent for

any $\tau_1 \in [0, 1]$. By differentiating with respect to τ_1 and using the Leibnitz rule, see (Billingsley, 2013), it is seen that,

$$\frac{-F'(\tau_1)}{1 - F(\tau_1)} = \frac{u_1'(\tau_1)}{u_2(\tau_1) - u_1(\tau_1)} \sim h(\tau_1), \quad \tau \in [0, 1]. \quad (35)$$

One can see that,

$$h(\tau_1) = \begin{cases} 0.5\tau_1^{-1}, & 0 < \tau_1 \leq \tau^*, \\ 0.5(1 - \tau_1)^{-1}, & \tau^* \leq \tau_1 < 1. \end{cases} \quad (36)$$

Thus, the distribution function is derived as

$$F(\tau_1) = 1 - e^{-H(\tau_1)}$$

and

$$H(\tau_1) = \int_0^{\tau_1} h(s) ds. \quad (37)$$

To make sure that Equation (37) is a proper integral, lower bounds 0 and 1 are replaced by θ and $(1 - \theta)$, respectively, for some positive small number $\theta > 0$. To numerically show that $F(\tau_1)$ is well defined, let $\tau^* = 0.25$, and $\theta = 0.01$. Then,

$$h(\tau_1) = \begin{cases} 0.5\tau_1^{-1}, & 0.01 < \tau_1 \leq 0.25, \\ 0.5(1 - \tau_1)^{-1}, & 0.25 \leq \tau_1 < 0.99. \end{cases} \quad (38)$$

Then, the survive function $1 - F(\tau)$ is given by,

$$1 - F(\tau) = \begin{cases} 0.1\tau^{-0.5}, & 0.01 < \tau \leq 0.25, \\ 0.2309\sqrt{1 - \tau}, & 0.25 < \tau \leq 0.99. \end{cases} \quad (39)$$

The density of mixture cumulative distribution function (Mix-CDF) $F(\tau)$ is given by,

$$f(\tau) = \begin{cases} 0.05\tau^{-1.5}, & 0.01 < \tau \leq 0.25, \\ 0.2309(1 - \tau)^{-0.5}, & 0.25 < \tau \leq 0.99. \end{cases} \quad (40)$$

$F(\tau)$ and related density (Mix-Dens), i.e. $f(\tau)$, are illustrated in Figure 3.

Alternatively, suppose that the ultimate estimation of the change is given by the mean of τ_1 and τ_2 . Hence, the expected payoff in this case is given by,

$$\begin{aligned} pay_1^* &= \int_0^1 u \left(\frac{\tau_1 + \tau_2}{2} \right) dF(\tau_2) \\ &= \int_0^{\tau_1} u_2 \left(\frac{\tau_1 + \tau_2}{2} \right) dF(\tau_2) \\ &\quad + \int_{\tau_1}^1 u_1 \left(\frac{\tau_1 + \tau_2}{2} \right) dF(\tau_2) \\ &= \int_0^{\tau_1} u_2 \left(\frac{\tau_1 + \tau_2}{2} \right) dF(\tau_2) \\ &\quad + \int_{\tau_1}^1 u_1 \left(\frac{\tau_1 + \tau_2}{2} \right) dF(\tau_2). \end{aligned} \quad (41)$$

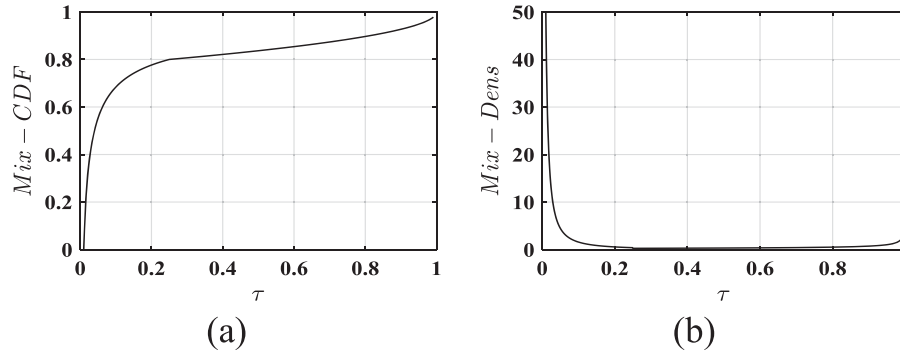


Figure 3. (a) Plot of mixture CDF and (b) plot of mixture density.

Let $\frac{\partial pay_1^*}{\partial \tau_1} = 0$. Then, it is seen that

$$F'(\tau_1)\{u_2(\tau_1) - u_1(\tau_1)\} + I + II = 0. \quad (42)$$

where

$$\begin{aligned} I &= \frac{1}{2} \int_0^{\tau_1} u_2' \left(\frac{\tau_1 + \tau_2}{2} \right) dF(\tau_2) \\ &= \frac{\tau_1}{2} \int_0^{\tau_1} u_2'(y) F'(2y - \tau_1) dy, \\ II &= \frac{1}{2} \int_{\tau_1}^1 u_1' \left(\frac{\tau_1 + \tau_2}{2} \right) dF(\tau_2) \\ &= \frac{1 + \tau_1}{2} \int_{\tau_1}^1 u_1'(y) F'(2y - \tau_1) dy, \end{aligned}$$

and $y = \frac{\tau_1 + \tau_2}{2}$.

It is easy to see that

$$I = \begin{cases} \frac{\varphi(1 - \tau^*)F(\tau_1)}{2}, & \tau_1 \leq \tau^*, \\ \frac{\varphi F(2\tau^* - \tau_1)}{2} - \frac{\varphi \tau^* F(\tau_1)}{2}, & \tau^* < \tau_1 \leq 2\tau^*, \\ \frac{-\varphi \tau^* F(\tau_1)}{2}, & \tau_1 > 2\tau^*, \end{cases}$$

$$II = \begin{cases} \frac{-\varphi(1 - \tau^*)(1 - F(\tau_1))}{2}, & \tau_1 \leq 2\tau^* - 1, \\ \frac{\varphi \tau^*}{2} - \frac{\varphi F(2\tau^* - \tau_1)}{2} + \frac{\varphi(1 - \tau^*)F(\tau_1)}{2}, & 2\tau^* - 1 < \tau_1 \leq \tau^*, \\ \frac{\varphi \tau^*(1 - F(\tau_1))}{2}, & \tau_1 > \tau^*. \end{cases} \quad (43)$$

Again, a differential equation is derived for F . Solving this equation, F is derived.

Proposition 3.2: The mixed Nash equilibrium distribution function F is given by

(a) When the ultimate change point is $\min(\tau_1, \tau_2)$, then

$$F(\tau_1) = 1 - e^{-H(\tau_1)}, \quad H(\tau_1) = \int_0^{\tau_1} h(s) ds, \quad (44)$$

$$\text{where } h(\tau_1) = \begin{cases} 0.5\tau_1^{-1}, & 0 < \tau_1 \leq \tau^*, \\ 0.5(1 - \tau_1)^{-1}, & \tau^* \leq \tau_1 < 1. \end{cases}$$

(b) When the ultimate change point is $0.5(\tau_1 + \tau_2)$, then F satisfies (42).

3.3. Differential game

Under AMOC hypothesis, a differential game (Bressan, 2010) is proposed based on $T_{n,\theta}^2$. It is solved using the Pontryagin maximum principle and its Nash equilibrium is derived. Consider $T_{n,\theta}^2$ and let the magnitude of change be positive, i.e. $\varphi > 0$. Define the process T_s as follows

$$T_s = \int_0^s \pi_x u_{[nx]}^n dx, \quad (45)$$

where $u_t^n = \sqrt{\lambda_t(1 - \lambda_t)}(\hat{\beta}_t - \hat{\beta}_t^*)$, where $\hat{\beta}_t$ and $\hat{\beta}_t^*$ are computed by players 1 and 2, respectively. The Mayer type differential game is as (Bressan, 2010),

$$\begin{aligned} \min J &= T_1, \\ T_s' &= \pi_s u_{[ns]}^n. \end{aligned} \quad (46)$$

where T_s' is derivative of T_s with respect to s . The Hamiltonian function H_s using co-state variable p_s is given by,

$$H = H_s = -p_s \pi_s u_{[ns]}^n. \quad (47)$$

It is seen that $\partial H / \partial T_s = p_s' = 0$ which shows that p_s is a constant. Since $\partial T_1 / \partial T_1 = p_1 = 1$, then $p_s = 1$ for all s . Also, using Bang-Bang control (Isermann, 2006), it is

seen that,

$$\pi_s = \begin{cases} 1, & \text{if } u_{[ns]}^n > 0, \\ 0, & \text{otherwise,} \end{cases} = \begin{cases} 1, & \text{if } \hat{\beta}_{[ns]} > \hat{\beta}_{[ns]}^*, \\ 0, & \text{otherwise.} \end{cases} \quad (48)$$

An equivalent form for π_s is given by,

$$\pi_s = \begin{cases} 1, & \text{if } \hat{\beta}_{[ns]} - \hat{\beta}_n > c, \\ 0, & \text{otherwise,} \end{cases} \quad (49)$$

where c denotes a constant number. To find c , under H_0 , let $P(\hat{\beta}_{[ns]} - \hat{\beta}_n > c) = \alpha$, for some predetermined significant level $1 - \alpha$. As $n \rightarrow \infty$, using asymptotic distributions in Section 2.3, with $g(u) = u$, then $\hat{\beta}_{[ns]} - \hat{\beta}_n \rightsquigarrow \frac{W(s) - sW(1)}{s} \sim N(0, \frac{1-s}{s})$. Thus, $c = z_\alpha \sqrt{\frac{1-s}{s}}$, where z_α is $(1 - \alpha)$ -th quantile of standard normal distribution. An alternative of c is zero, since under H_0 , then $E(\hat{\beta}_{[ns]} - \hat{\beta}_n) = 0$. Let $t_* = \inf\{t, \hat{\beta}_t - \hat{\beta}_t^* > 0\}$. Since $\hat{\beta}_t - \hat{\beta}_t^*$ is too close to its expectation (Bai, 1994), then $t_* = \inf\{t, E(\hat{\beta}_t - \hat{\beta}_t^*) > 0\}$. First assume that $t \leq t^*$. Then,

$$E(\hat{\beta}_t - \hat{\beta}_t^*) = \frac{\sum_{i=t+1}^n x_i^2}{\sum_{i=t+1}^n x_i^2} \varphi > 0 \quad (50)$$

which is maximised at t^* . This fact leads to $t_* = t^*$. Indeed, at $t = t^*$ no player is willing to change its strategy (to choose another point as a change point). This shows that the Nash equilibrium happens at $t = t^*$. The same result is also obtained when $t \geq t^*$ is considered.

Proposition 3.3: Considering the process T_s as (45), the differential game solution is given by (49).

Now to illustrate the differential game approach, two simple examples for uniformly distributed random states and first order state feedback system are studied.

- (a) For $n = 1000$, $t^* = 200$, $b_1 = 1$, $b_2 = 5$, $\sigma_\varepsilon = 0.1$ and x_t 's are the sorted sequence of n independent and uniformly distributed variables on $(0, 1)$, the time series plot of $\hat{\beta}_{[ns]} - \hat{\beta}_n$ is shown in Figure 4.
- (b) Let $n = 1000$, $t^* = 200$, $b_1 = 1$, $b_2 = 5$, $\sigma_\varepsilon = 0.1$ and x_t 's come from correlated states $x_t = \alpha x_{t-1} + \gamma u_t + e_t$, and $u_t = Kx_t$, with $\alpha = 0.1$, $\gamma = 0.5$ and $K = 0.2$, then, the time series plot of $\hat{\beta}_{[ns]} - \hat{\beta}_n$ is shown in Figure 5.

In the unknown states cases, x_t 's are estimated by the Kalman filter and, accordingly, the differential game is presented in Section 4.2.

3.4. Epidemic game

The epidemic change point is a special case of multiple change point model where $\beta_t = b_i$ for $t_i^* + 1 \leq t \leq t_{i+1}^*$

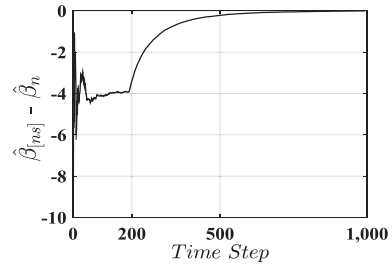


Figure 4. Time series plot of $\hat{\beta}_{[ns]} - \hat{\beta}_n$, known uniform states.

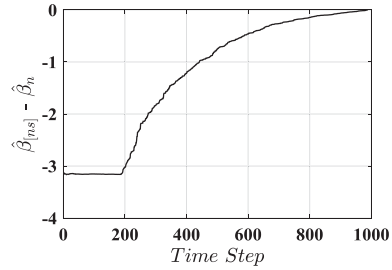


Figure 5. Time series plot of $\hat{\beta}_{[ns]} - \hat{\beta}_n$, known correlated states.

with $i = 0, \dots, R - 1$, $t_0^* = 0$, where R denotes the number of change points. In the epidemic case, R is kept fixed at 2. The regular way to detect change points t_i^* , $i = 1, 2, \dots, R - 1$, is first to estimate R and then estimating t_{R-1}^* and to move backward to t_1^* . Here, the two-way game theoretic solution to the epidemic change problem is proposed. Consider (1). Since, β_t plays the role of the mean of y_t , to detect two change points, two CUMSUM partial sum processes $u_n^1(y, \tau_1, \tau_2)$ and $u_n^2(y, \tau_1, \tau_2)$ are as follows

$$\begin{aligned} u_n^1(y, \tau_1, \tau_2) &= \frac{1}{n} \sum_{i=1}^{[n\tau_1]} (y_i - \bar{y}_{[n\tau_2]}), \\ u_n^2(y, \tau_1, \tau_2) &= \frac{1}{n} \sum_{i=1}^{[n\tau_2]} (y_{n-i+1} - \bar{y}_{[n\tau_1]}^*), \end{aligned} \quad (51)$$

for $0 < \tau_1 \leq \tau_2 < 1$. Here, $\bar{y}_{[n\tau_1]}^*$ is the mean of y_{n-i+1} , $i = 1, 2, \dots, [n\tau_1]$. While detection of τ_1 , given that τ_2 is known, the stochastic process $|u_n^1(y, \tau_1, \tau_2)|$ is maximised by player 1 and for detecting of τ_2 , given τ_1 , the process $|u_n^2(y, \tau_1, \tau_2)|$ is maximised by player 2. This problem defines a stochastic dynamic game for two players with payoff functions $|u_n^i(y, \tau_1, \tau_2)|$, $i = 1, 2$, respectively.

As follows, the Nash equilibrium of the two-way game is found. First notice that $u_n^i(y, \tau_1, \tau_2)$ behaves such that its mean $\mu_n^i(\tau_1, \tau_2) \approx E(u_n^i(y, \tau_1, \tau_2))$. To see this, notice that,

$$u_n^i(y, \tau_1, \tau_2) = \mu_n^i(\tau_1, \tau_2) + u_n^i(\varepsilon, \tau_1, \tau_2), \quad i = 1, 2. \quad (52)$$

Then, as $n \rightarrow \infty$, using the Donsker theorem (Billingsley, 2013), it is seen that,

$$\begin{aligned} n^{1/2} u_n^1(\varepsilon, \tau_1, \tau_2) &\rightsquigarrow W(\tau_1) - \frac{\tau_1}{\tau_2} W(\tau_2), \\ n^{1/2} u_n^2(\varepsilon, \tau_1, \tau_2) &\rightsquigarrow W^*(\tau_2) - \frac{\tau_2}{1-\tau_1} W^*(\tau_1). \end{aligned} \quad (53)$$

Here, notation $W(t)$ stands for standard Brownian motion on $[0,1]$ and $W^*(t) = W(1) - W(t)$. Also, notice that,

$$\begin{aligned} \max_{\theta \leq \tau_1 \leq \tau_2 \leq 1-\theta} \left| W(\tau_1) - \frac{\tau_1}{\tau_2} W(\tau_2) \right| &= O_p(1), \\ \max_{\theta \leq \tau_1 \leq \tau_2 \leq 1-\theta} \left| W^*(\tau_2) - \frac{\tau_2}{1-\tau_1} W^*(\tau_1) \right| &= O_p(1). \end{aligned} \quad (54)$$

Thus, $u_n^i(y, \tau_1, \tau_2)$, $i = 1, 2$ behaves similar to its mean, since

$$\begin{aligned} \max_{\theta \leq \tau_1 \leq \tau_2 \leq 1-\theta} |u_n^i(y, \tau_1, \tau_2) - \mu_n^i(\tau_1, \tau_2)| \\ = O_p\left(n^{-\frac{1}{2}}\right), \quad i = 1, 2. \end{aligned} \quad (55)$$

Hereafter, the Nash equilibriums are sought. One can see that $\mu_1(\tau_1, \tau_2) = 0$ if $\tau_2 \leq \tau_1^*$. When, $\tau_1^* \leq \tau_2 \leq \tau_2^*$, then,

$$\mu_1(\tau_1, \tau_2) = \begin{cases} -\varphi \tau_1 \left(1 - \frac{\tau_1}{\tau_2}\right), & \text{if } \tau_1 \leq \tau_1^*, \\ -\varphi \tau_1^* \left(1 - \frac{\tau_1}{\tau_2}\right), & \text{if } \tau_1 > \tau_1^*. \end{cases} \quad (56)$$

When $\tau_2^* \leq \tau_2 \leq 1$, then,

$$\begin{aligned} \mu_1(\tau_1, \tau_2) \\ = \begin{cases} -\varphi \frac{\tau_1}{\tau_2} (\tau_2^* - \tau_1^*), & \text{if } \tau_1 \leq \tau_1^*, \\ -\varphi \begin{cases} \tau_1^* \left(1 - \frac{\tau_1}{\tau_2}\right) \\ -\tau_1 \left(1 - \frac{\tau_2^*}{\tau_2}\right) \end{cases}, & \text{if } \tau_1^* \leq \tau_1 \leq \tau_2^*, \\ \varphi \left(1 - \frac{\tau_1}{\tau_2}\right) (\tau_2^* - \tau_1^*), & \text{else } \tau_1 > \tau_2^*. \end{cases} \end{aligned} \quad (57)$$

By changing the τ_1 to τ_2 and t_1^* to t_2^* , the mean function $\mu_2(\tau_1, \tau_2)$ is derived. The best response of player 1 when the player 2 considers the change as τ_2 is given by,

$$B_1(\tau_2) = \begin{cases} [\theta, \tau_2], & \theta \leq \tau_2 \leq \tau_1^*, \\ \tau_1^*, & \tau_1^* \leq \tau_2 \leq \tau_2^*, \\ \tau_1^*, & \tau_2^* \leq \tau_2 \leq 1 - \theta. \end{cases} \quad (58)$$

If it is assumed that $\mu_1(\tau_1, \tau_2) \neq 0$, then $B_1(\tau_2) = \tau_1^*$. Similarly, $B_2(\tau_1) = \tau_2^*$. This fact shows that the Nash equilibrium happens at (τ_1^*, τ_2^*) . The following proposition summarises the above discussion.

Proposition 3.4: *The Nash equilibriums of two-way FDI game occurs at the actual change points (τ_1^*, τ_2^*) .*

4. Two-way FDI: unknown states

The unknown states case as an inevitable practical issue (Isermann, 2006) is considered here. Indeed, in Sections 2 and 3, the states are needed to be known. So, in this section, previous results and approaches are modified to be applicable for unknown state situations. LMI and Kalman filter methods are utilised to tackle this problem.

4.1. LMI application

Here, without loss of generality, assume that the magnitude of change is negative, i.e. $\varphi < 0$. According to the results of Section 2, the null hypothesis H_0 is rejected (against AMOC alternative hypothesis H_1) for large value of test statistic $\max_t J(x, t)$, where

$$J(x, t) = \lambda_t^{0.5} (1 - \lambda_t)^{-0.5} (\hat{\beta}_t - \hat{\beta}_n), \quad (59)$$

where $\lambda_t = \frac{s_t}{s_n}$, $s_t = \sum_{i=1}^t x_i^2$ for $t = 1, 2, \dots, n$, and $x = \{x_t, t \geq 1\}$, see Section 2. Values of $J(x, t)$'s are attainable if the x_t 's are known. This approach is referred to as the player test statistic in Section 2. For the unknown states cases, following (Chung and Speyer, 1998) and using a conservative approach, the null hypothesis H_0 is rejected if,

$$\min_x \max_t J(x, t) \geq d, \quad (60)$$

for some thresholds d 's. These d 's are computed using the null distribution of $\min_x \max_t J(x, t)$, such that

$$P_{H_0}(\min_x \max_t J(x, t) \geq d) = \alpha, \quad (61)$$

for some desired significant level $1 - \alpha$. Following Section 2, when the above-mentioned method is repeated for two players 1 and 2, a two-way FDI is made. To make inference, the asymptotic distribution of $\min_x \max_t J(x, t)$ is needed. However, an alternative approach is the use of the LMI technique. H_0 is rejected if for all x 's

$$\max_t J(x, t) \geq d \quad (62)$$

Hence, H_0 is retained (not rejected yet) if $d - \max_t J(x, t) \leq 0$, for some x 's. This condition defines $[n(1 - \theta)] - [n\theta]$ numbers of LMI's for each t . If the above inequality is solved by LMI and some x 's are found, then H_0 is not rejected. However, there is no guarantee that the x 's found by LMI are the actual x 's. To overcome this difficulty, using the Kalman filter, the actual x 's are estimated and compared with the LMI x 's by some criteria like mean square error and mean absolute percentage error. If these two series of x 's are close, then it is concluded that there is a change at the actual x 's.

To simplify the LMI problem, notice that the maximum of $\lambda_t^{0.5}(1-\lambda_t)^{-0.5}$ is $\sqrt{\vartheta/(1-\vartheta)}$, for some ϑ where $0 < \lambda_t < \vartheta$, then the H_0 is retained if

$$d' - \max_t(\hat{\beta}_t - \hat{\beta}_n) \leq 0, \quad (63)$$

where $d' = \sqrt{(1-\vartheta)/\vartheta}d$. This is an LMI solution. Therefore, the LMI is applied to find x 's.

Hereafter, a different formulation of LMI is presented. Suppose that it is desired to test if there is a change at a specified point t . The null hypothesis H_0 is rejected if $J(x, t) > c_t$, for some threshold c_t 's. One can see that it is equivalent to say that

$$\left(\sum_{i=1}^t x_i y_i\right) \left(\sum_{i=1}^n x_i^2\right) - \left(\sum_{i=1}^n x_i y_i\right) \left(\sum_{i=1}^t x_i^2\right) > c_t s_n^2 \sqrt{\lambda_t(1-\lambda_t)}. \quad (64)$$

An alternative format of (64) is as,

$$\left(\sum_{i=1}^t x_i^2 \frac{y_i}{x_i}\right) \left(\sum_{i=1}^n x_i^2\right) - \left(\sum_{i=1}^n x_i^2 \frac{y_i}{x_i}\right) \left(\sum_{i=1}^t x_i^2\right) > q_t, \quad (65)$$

where $q_t = c_t s_n^2 \sqrt{\lambda_t(1-\lambda_t)} \leq 0.5 c_t s_n^2$. Assume that

$$F_i = \begin{cases} \begin{bmatrix} \frac{y_i}{x_i} & \frac{y_i}{x_i} \\ 1 & 1 \end{bmatrix}, & i = 1, \dots, t \\ \begin{bmatrix} 0 & \frac{y_i}{x_i} \\ 0 & 1 \end{bmatrix}, & i = t+1, \dots, n \end{cases}. \quad (66)$$

Then, inequality $\left(\sum_{i=1}^t x_i^2 \frac{y_i}{x_i}\right) \left(\sum_{i=1}^n x_i^2\right) - \left(\sum_{i=1}^n x_i^2 \frac{y_i}{x_i}\right) \left(\sum_{i=1}^t x_i^2\right) > 0.5 c_t s_n^2$ can be represented by $\begin{bmatrix} \sum_{i=1}^n x_i^2 F_i \\ I \end{bmatrix} < 0$ which defines a LMI problem. Here, unknown x_i 's of F_i are estimated by Kalman filtering and I is the identity matrix.

4.2. Kalman filter

Here, via elaborating an example, the application of the Kalman filter to estimate the unknown states is described. Then, the differential game of Section 3.3 is applied for the unknown states case. It is seen that the differential game approach by using Kalman estimated states works well. A similar approach under the Bayesian setting for sensor FDI has been studied in Habibi, Howard, and Habibi (2017a).

Consider a servo mechanism, whose transfer function $G(s)$ is as,

$$G(s) = \frac{1}{s(s+1)(s+2)}. \quad (67)$$

The reference input r is a unit step. The desired closed loop poles are chosen to be at $s = -2 \pm j2\sqrt{3}$ and $s = -10$. The state feedback controller is utilised to place the poles as desired values. The state space representation of this system is

$$\begin{aligned} \dot{x}_t &= Ax_t + bu_t, \\ y_t &= c_t x_t + \varepsilon_t, \end{aligned} \quad (68)$$

where $x_t = [x_{1t} x_{2t} x_{3t}]^T$, $c_t = [\beta_t \ 0 \ 0]$, at which

$$\beta_t = \begin{cases} 1, & t \leq t^*, \\ 5, & t > t^*, \end{cases} \quad (69)$$

where $t^* = 200$. The control term is given by $u_t = -kx_t$, $k = [160 \ 54 \ 11]$. Coefficients of the state equation are $A = \begin{bmatrix} 0 & 1 & 0 \\ 0 & 0 & 1 \\ 0 & -2 & -3 \end{bmatrix}$, $b = [001]^T$. Vectors and matrices are represented by bolded small and capital letters, respectively. Here, ε_t 's are independent random variables with common normal distribution $N(0, 0.25)$.

The Kalman filter, which is used to estimate the states, is designed as

$$\hat{x}_t = A\hat{x}_t + bu_t + k_f(y_t - \hat{y}_t), \quad (70)$$

where \hat{x}_t , $\hat{y}_t = \hat{x}_{1t}$ and k_f are the Kalman estimates of states, output and gain, respectively.

The vector c_t of the Kalman filter is $[1 \ 0 \ 0]$, considering a latent fault in the sensor. On the other hand, to hold $x_{1t} = \hat{x}_{1t}$, as the goal of the Kalman filter, the latent coefficient β_t should be applied in vector c_t of the Kalman filter. Accordingly, the Kalman filter (70) is modified as,

$$\hat{x}_t = A\hat{x}_t + bu_t + k_f(y_t - \beta_t \hat{x}_{1t}). \quad (71)$$

So, by selecting the appropriate estimator gain, the estimated state via the Kalman filter, i.e. \hat{x}_{1t} , will be close optimally to the term of x_{1t}/β_t . Consequently, it can be concluded that the estimated state is not similar to the state x_1 , but rather to the x_{1t}/β_t term, in which the coefficient β_t is present (Habibi, Howard, & Habibi, 2017a).

The differential game of Section 3 utilises the plot of $\hat{\beta}_{[nl]} - \hat{\beta}_n$, $0 < l < 1$, for FDI purposes. This plot for dynamic system (68) with a sensor fault (69), using Kalman estimations of states instead of actual unknown states, is shown in Figure 6. It is seen that the differential game method is also applicable in the unknown states case. It should be noted that the data before the change

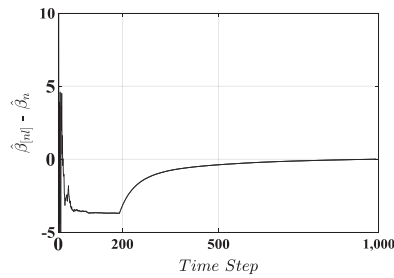


Figure 6. Time series plot of $\hat{\beta}_{[n]} - \hat{\beta}_n$, Kalman estimation.

point has negative effect on rate of convergence. Hence, a delay is observed. This problem can be removed via the windowed coefficient estimation, i.e. rolling analysis, which is surveyed as an illustrative example in Section 5.2, Example 5.4.

5. Illustrative examples, practical simulation and comparison

In this section, initially, the finite sample distribution of the test statistic is simulated. Then, four illustrative examples are given with different fault scenarios to investigate the different characteristics of the two-way FDI method. Finally, the integrated servo mechanism with unknown states, as a practical example, is studied to evaluate the superiority of the proposed schemes.

5.1. Finite sample distributions

Here, the finite sample quantiles d' of test statistic $T_{n,\theta}^1$ are derived at which $T_{n,\theta}^1 > d$ rejects the null hypothesis H_0 of no change. Although, the large sample quantiles are derived in Section 2.3, however, often, in practical situations, finite samples are available. So finite sample quantiles are beneficial to be studied. Values of d' s are derived for various selections of sample size n , variance σ_ε^2 , and states x_t 's. Three cases (a)–(c) are given, as follows.

First, suppose that states x_t 's are sorted n independent uniform random variables with common uniform distribution on $(0,1)$. The sensor parameter $b_1 = 1$. Let $\theta = 0.1$. Table 3 gives the Monte Carlo estimation (based on 1000 repetitions) of the 0.99-th quantile d for various values of n and σ_ε^2 .

Table 3. The 0.99-th quantile d , uniform states.

		σ_ε				
		0.01	0.1	0.5	1	2
n	10	0.01434	0.14342	0.71714	1.43428	2.86856
	20	0.01143	0.11432	0.57164	1.14323	2.28658
	30	0.00998	0.09989	0.49946	0.99893	1.99786
	40	0.00809	0.08093	0.40468	0.80936	1.61873
	50	0.00784	0.07843	0.39219	0.78438	1.56876

Table 4. The 0.99-th quantile d , known states.

		σ_ε				
		0.01	0.1	0.5	1	2
n	10	0.01247	0.12476	0.62381	1.24761	2.4952
	20	0.00941	0.094051	0.47025	0.94051	1.8811
	30	0.00615	0.061525	0.30762	0.61525	1.2305
	40	0.00485	0.04856	0.24281	0.48562	0.9712
	50	0.00387	0.03873	0.19365	0.38731	0.7746

Table 5. The 0.99-th quantile d , Kalman filtering.

		σ_ε				
		0.01	0.1	0.5	1	2
n	10	0.0112	0.1171	0.7476	1.9964	3.4734
	20	0.0080	0.0883	0.4778	1.0493	1.9838
	30	0.0069	0.0717	0.3527	0.6954	1.2143
	40	0.0061	0.0628	0.3132	0.6310	1.1916
	50	0.0056	0.0545	0.2841	0.5917	1.1449

Here, the finite sample quantiles are given for correlated states. Again, suppose that $b_1 = 1$, and that states x_t 's come from $x_t = \alpha x_{t-1} + \gamma u_t + e_t$, where e_t is normal standard random variable, $u_t = Kx_t$, with $\alpha = 0.1$, $\gamma = 0.5$ and $K = 0.2$. Let $\theta = 0.1$. It is assumed e_t and ε_t are independent. Table 4 gives the 0.99-th quantile d for various values of n and σ_ε^2 .

Now assume that states x_t 's are unknown and estimated by the Kalman filter. Let $\theta = 0.1$. Table 5 gives the mentioned quantiles for this case. It is worth noting that in both known and unknown cases, the d 's are similar.

Finite sample $(1 - \zeta)\%$ quantiles of $T_{n,\theta}^2$, for $n = 50$, $\theta = 0$, $b_1 = 1$, $\sigma_\varepsilon = 0.2$, and $\pi_t = 1$ for $t \in (0, 1)$, when the states are sorted, uniform observations in $(0, 1)$, are 0.07594, 0.06578 and 0.05703 for $\zeta = 0.01, 0.025$ and 0.05 , respectively. When, $x_t = \alpha x_{t-1} + \gamma u_t + e_t$, where e_t 's are normally distributed variables with zero mean and standard deviation 1, then mentioned quantiles are 0.0418, 0.0374 and 0.03345 for $\zeta = 0.01, 0.025$ and 0.05 , respectively.

Comparing Tables 3–5, almost in all cells, the smallest, largest and middle quantiles are known, uniform and Kalman states quantiles, respectively. As expected, larger σ_ε leads to larger quantiles. Also, for larger n , quantiles converge to constant limiting value. The 99-th quantiles of known states are illustrated in Figure 7. For two other quantiles similar figure can be obtained.

5.2. Illustrative examples

Here, four illustrative examples are given. The first example computes the best response functions (15) of both players and the Nash equilibrium is derived. To show that the considered fault model (3) and the proposed FDI scheme is applicable in other fault models, sensor bias/fixed output and epidemic changes are studied in the

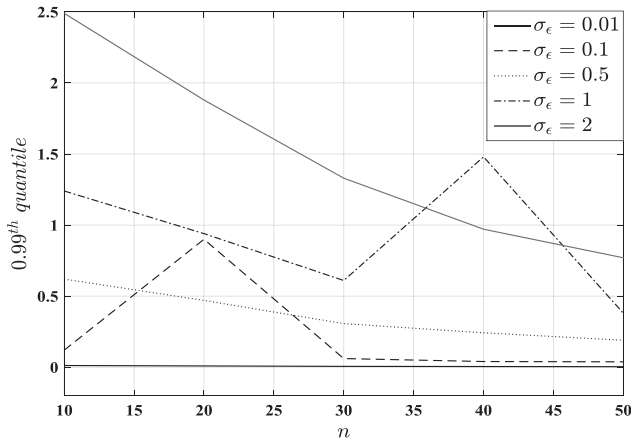


Figure 7. 0.99-th quantiles of known states.

second and third examples, respectively. The player test statistics and generally, game theoretic tools are obtained using the regular least square estimation of β_t . However, this estimation is disturbed with the past observations and this fact induces delays in fault diagnosis, as described in Section 4.2. To overcome this difficulty, the rolling estimations are used. So, in the last example the rolling estimation of a sensor coefficient at the change point is surveyed.

Example 5.1 (Best response functions.): Assuming the ultimate change is $\min(t, s)$, the best response functions of both players are given by (15)

$$\begin{aligned} B_1(s) &= \operatorname{argmax}_{1 \leq t \leq n} |u_{\min(t,s)}^n|, \\ B_2(t) &= \operatorname{argmax}_{1 \leq s \leq n} |u_{\min(t,s)}^n|. \end{aligned} \quad (72)$$

Also, these functions are B_1^* and B_2^* , using the average $0.5(s + t)$ as the ultimate estimation of change, that is,

$$\begin{aligned} B_1^*(s) &= \operatorname{argmax}_{1 \leq t \leq n} |u_{0.5(s+t)}^n|, \\ B_2^*(t) &= \operatorname{argmax}_{1 \leq s \leq n} |u_{0.5(s+t)}^n|, \end{aligned} \quad (73)$$

where $u_t^n = \sqrt{\lambda_t(1 - \lambda_t)^{-1}}(\hat{\beta}_t - \hat{\beta}_n)$ and $s_t = \sum_{i=1}^t x_i^2$ and $\lambda_t = \frac{s_t}{s_n}$, $t = 1, 2, \dots, n$.

As follows Nash equilibriums are derived in three cases (a)-(c).

First, it is supposed that the x_t 's are sorted $n = 100$ independent uniform random variables with common uniform distribution on $(0,1)$. The change occurs at $t^* = 30$ where $b_1 = 1$, $b_2 = 3$ and $\sigma_\epsilon = 0.1$. Figure 8 shows the graphs of functions B_1 and B_2 which are the same. The graphs of B_1^* and B_2^* are also given in Figure 9. Both Figures 8 and 9 show that the Nash equilibrium occurs at $t = 30$. Although, apparently, Figure 9 shows that the change has occurred at $t = 60$, however, because of the

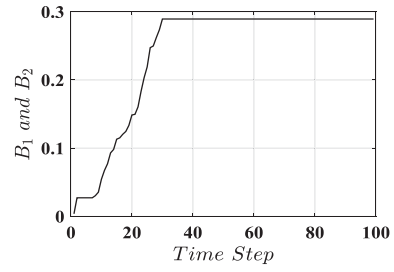


Figure 8. Graphs of functions B_1 and B_2 for uniform states, Illustrative Example 5.1 (a).

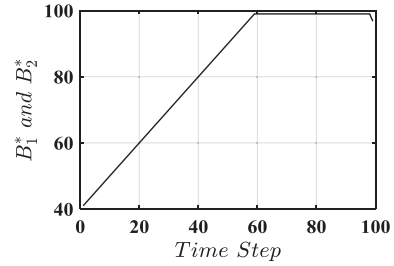


Figure 9. Graphs of functions B_1^* and B_2^* for uniform states, Illustrative Example 5.1 (a).

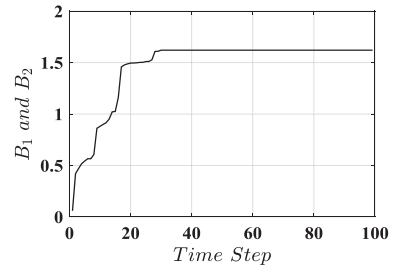


Figure 10. Graphs of functions B_1 and B_2 for known correlated states, Illustrative Example 5.1 (b).

functional form of the argument $0.5(t + s)$, it should be divided by 2 to derive the actual change point $t = 30$.

Again, suppose that $b_1 = 1$, $b_2 = 3$, $n = 100$, $t^* = 30$, and $\sigma_\epsilon = 0.1$. However, states x_t 's come from $x_t = \alpha x_{t-1} + \gamma u_t + e_t$, and $u_t = Kx_t$, with $\alpha = 0.1$, $\gamma = 0.5$ and $K = 0.2$. For this example, Figure 10 shows the plots of functions B_1 and B_2 which are the same. Also, the graphs of B_1^* and B_2^* are given in Figure 11. Both Figures 10 and 11, show that the Nash equilibrium occurs at $t = 30$. Similar to the reasoning of Figure 9, $t = 60$ should be divided by 2 to derive the actual change point $t = 30$.

Figure 12 shows the graphs of functions B_1 and B_2 when the Kalman filtering is used to estimate the states in part (b). Again, it is seen that the Nash equilibrium occurs at $t = 30$.

Example 5.2 (Sensor bias and sensor fixed output.): These are two special cases of systems at which a fixed number (bias) is added to the output of a system (referred

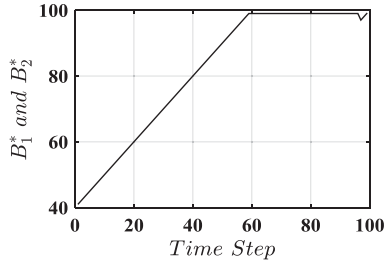


Figure 11. Graphs of functions B_1^* and B_2^* for known correlated states, Illustrative Example 5.1 (b).

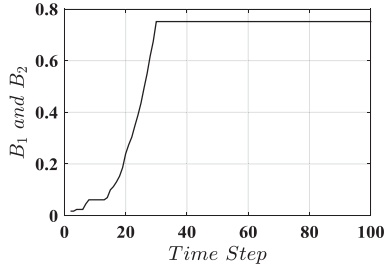


Figure 12. Graphs of functions B_1 and B_2 , Kalman estimation of correlated states, Illustrative Example 5.1 (c).

to as sensor bias) and the output of a system is fixed (referred to as sensor fixed output), see (Isermann, 2006). Consider cases (a)–(b), as follows.

For the sensor bias case, let

$$y_t = x_t + \omega_t + \varepsilon_t, t = 1, 2, \dots, 1000, \quad (74)$$

where x_t 's is a sorted sequence of 1000 random numbers uniformly distribution on (0,1), and

$$\omega_t = \begin{cases} 0, & t \leq 450, \\ 1, & t \geq 451. \end{cases} \quad (75)$$

Here, to study the change in the bias term of the system, the β_t is assumed zero. Error terms ε_t 's come from normal distribution with zero mean and standard deviation $\sigma_\varepsilon = 0.5$.

To apply the two-way FDI, here, it is enough to let

$$z_t = y_t - x_t = (\omega_t \times 1) + \varepsilon_t. \quad (76)$$

That is, the coefficient of the fixed sensor which is 1, suddenly changes at an unknown time point. This is a regression model similar to model (1). It is not difficult to see that

$$\hat{\beta}_t = \bar{z}_t \text{ and } u_t^n = \sqrt{\frac{t}{n-t}}(\bar{z}_t - \bar{z}_n) \quad (77)$$

Figure 13 shows the time series of $|u_t^n|$ indicating there is a change at $t = 450$. It is seen that the maximum of this plot

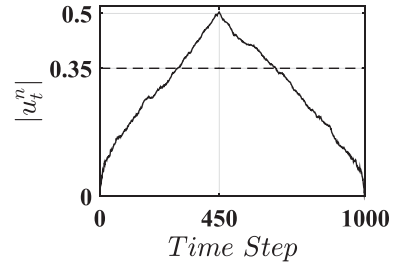


Figure 13. Time series of $|u_t^n|$, Illustrative Example 5.2 (a).

occurs at the actual change point out of the 95% quantile boundary, i.e. 0.35. Thus, similar to the arguments of the previous Section, the Nash equilibrium occurs at $t = 450$, i.e. at the true change point.

(b) For the fixed output case, assume that

$$y_t = \beta_t x_t + w_t + \varepsilon_t, t = 1, 2, \dots, 1000 \quad (78)$$

where $\beta_t = 0$ and $w_t = 1$ for $t \leq 450$ and $\beta_t = 0$ and $w_t = 2$ for $t > 450$. It should be noted that β_t is selected to be 0 to make the effect of the bias apparent. Here, u_t^n of formula (13) reduces to

$$u_t^n = \sqrt{\frac{t}{n-t}}(\bar{y}_t - \bar{y}_n), \quad (79)$$

which is a suitable process to detect the change point. Obviously, the two-way FDI performs well, in this case.

For another example, consider the following case.

$$y_t = \beta_t x_t + w_t + \varepsilon_t, t = 1, 2, \dots, 1000 \quad (80)$$

where $\beta_t = 0$ and $w_t = 1$ for $t \leq 450$ and $\beta_t = 1$ and $w_t = 2$ for $t > 450$. Here,

$$u_t^{n,*} = \sqrt{\frac{\lambda_t}{1-\lambda_t}}(\hat{\beta}_t^* - \hat{\beta}_n^*), \quad (81)$$

where $\hat{\beta}_t^* = \sum_{i=1}^t x_i(y_i - \bar{y}) / \sum_{i=1}^t x_i^2$. Here, ε_t 's are normal random variables with zero mean and standard deviation 0.1. Figure 14 shows the time series plot of $|u_t^{n,*}|$ which shows the change point at $t = 450$ out of the 95% quantile boundary, i.e. 0.86. In this case, a two-step procedure is used to detect changes in both parameters β_t and w_t . As soon as the change in β_t is detected, to detect the change in w_t , then let $z_t^* = y_t - \beta_t x_t$ and use the process

$$u_t^{n,**} = \sqrt{\frac{t}{n-t}}(\bar{z}_t^* - \bar{z}_n^*) \quad (82)$$

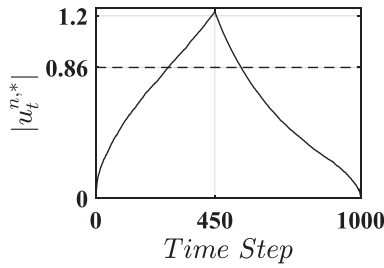


Figure 14. Time series of $|u_t^{n,*}|$, Illustrative Example 5.2 (b).

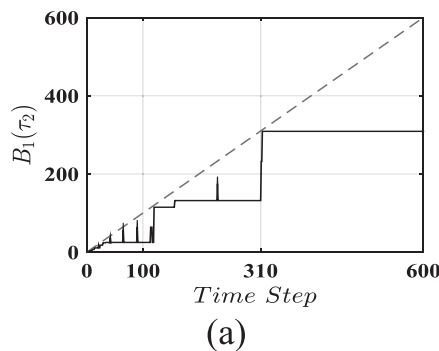
Example 5.3 (Epidemic change.): The epidemic change point is a special pattern of a multiple change point problem. Here, there are three segments (two change points) and the parameters of interest are the same for the first and third segments while the parameter in the middle segment has a different value. The epidemic pattern occurs in many fields such as medicine (influenza epidemics), meteorology (weather conditions, pollution), and seismology (earthquake), see (Habibi, et al., 2005).

In this example, following (51), let $n = 600$, $[n\tau_1] = 310$, $[n\tau_2] = 400$, $\sigma_\varepsilon = 0.1$ and, as discussed in Section 3, let $x_t = 1$ for all t 's. The change in β_t is as

$$\beta_t = \begin{cases} 1 & 1 \leq t \leq 310, \\ 3.25 & 311 \leq t \leq 400, \\ 1 & 401 \leq t \leq 600. \end{cases}, \quad (83)$$

Considering (51), the payoff functions of players 1 and 2 are given as

$$\begin{aligned} u_1(\tau_1, \tau_2) &= \frac{1}{n} \sum_{i=1}^{[n\tau_1]} (y_i - \bar{y}_{[n\tau_2]}), \\ u_2(\tau_1, \tau_2) &= \frac{1}{n} \sum_{i=1}^{[n\tau_2]} (y_{n-i+1} - \bar{y}_{[n\tau_1]}^*), \end{aligned} \quad (84)$$



respectively. The best response of player 1 when the player 2 chooses the strategy τ_2 is,

$$B_1(\tau_2) = \begin{cases} h(\tau_1), & \text{if } \tau_2 \leq \frac{310}{600}, \\ \frac{310}{600}, & \text{if } \frac{310}{600} < \tau_2 \leq \frac{400}{600}, \\ \frac{310}{600} \text{ or } \frac{400}{600}, & \text{if } \tau_2 > \frac{400}{600}, \end{cases} \quad (85)$$

where h is often a non-decreasing function of τ_1 (see, Figure 15(a, b)). In the third row of formula (85), the best response of player 1 is $310/600$ or $400/600$ depending if $u_1(310/600, \tau_2) > u_1(400/600, \tau_2)$ is true or not. However, it is true that the $B_1(\tau_2)$ is a step function after $310/600$ and its value is $310/600$ (see, Figure 15(a, b)). A similar fact is true for $B_2(\tau_1)$. To find the Nash equilibrium estimate of the first change point (which is $\frac{310}{600}$, actually), it is enough to find the intersection of. and line $[n\tau_1] = [n\tau_2]$. The intersection of $B_2(\tau_1)$ and line $\tau_1 = \tau_2$ gives the Nash equilibrium estimate of the second change point with actual value $\frac{400}{600}$. Figure 15(a, b) show the best response functions $B_1([n\tau_2])$ and $B_2([n\tau_1])$, respectively. Figure 15(a) indicates that there exists a change at time 310 and Figure 15(b) implies that there is another change at time $600 - 200 = 400$.

Example 5.4 (Rolling sensor estimate.): The rolling analysis is applied for capturing the instability of model parameters over time. It is an important technique widely used in financial time series analysis, see (Alexander, 2001) and references therein. Rolling sensor coefficients are the least square estimates of β_t computed using windowed samples. The data in the i -th sample is indexed by $i = t - l + 1, \dots, t$. The rolling estimations of β_t over a rolling window of size l is given by

$$\hat{\beta}_{\text{rolling},t} = \hat{\beta}_{l,t} = \frac{\sum_{i=0}^l x_{t-i} y_{t-i}}{\sum_{i=0}^l x_{t-i}^2}. \quad (86)$$

Under H_0 and AMOC model, then $E(\hat{\beta}_{l,t}) = b_1, t = 1, \dots, n$. This fact motivates one to use the CUMSUM $\hat{\beta}_{l,t}$, as a useful tool for change point detection. Similar

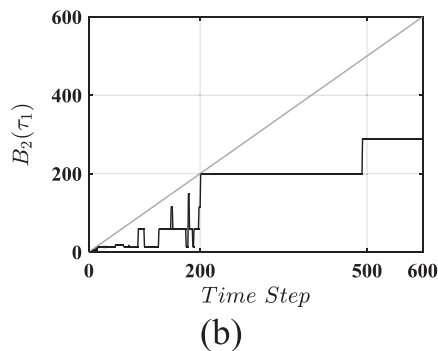


Figure 15. (a) Plots of $B_1(\tau_2)$ and (b) $B_2(\tau_1)$, Illustrative Example 5.3.

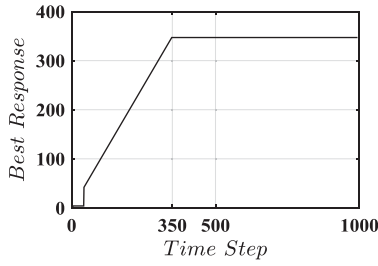


Figure 16. Best response function of both players, Illustrative Example 5.4.

to the previous Section, the utility function of player 1 is given by,

$$u_1(\tau) = \frac{1}{n} \sum_{i=1}^{[n\tau]} (\hat{\beta}_{l,t} - \bar{\hat{\beta}}), \quad (87)$$

where $\bar{\hat{\beta}}$ is the sample mean of $\hat{\beta}_{l,t}$, $i = 1, 2, \dots, n-l$. To obtain the utility function of the second player, it is enough to calculate the rolling estimate of length l using observations (x_{n-i+1}, y_{n-i+1}) , $i = 1, \dots, n$ and then compute the corresponding CUMSUM method. The best response functions of both players are plotted in Figure 16. Here, $n = 1000$, $t^* = 350$, $b_1 = 1$, $b_2 = 2.67$, $\sigma_\varepsilon = 0.1$ and x_t 's are sorted uniform variables on $(0,1)$. The length of the rolling window is $l = 10$. This shows that the Nash equilibrium estimation is the actual change point.

5.3. Practical example and comparison

In this section, the servo mechanism system, as introduced in Section 4.2, is considered to evaluate the performance of the two-way FDI method. Also, a comparison with CUMSUM method, as a one of the widely used FDI approaches (Isermann, 2006), is made to verify the advantages and benefits of the two-way FDI method. Here, the states x_t 's are assumed unknown, which is the case in most practical dynamic systems. Hence, as explained in Section 4.2, the Kalman filter is utilised to estimate the x_t 's. The servo mechanism considered in this section, is an integrated system, i.e. the output of a system is not observed directly, and instead a cumulative level of it exists for FDI purposes, inevitably. Integrated volatility and ice-core data on oxygen isotopes are two examples of integrated systems (Baltazar-Larios and Sørensen, 2010). In the integrated system, the available output is the integration of y_t as

$$y_t^* = \int_0^t y_s ds. \quad (88)$$

As the output y_t is integrated and hence it is non-stationary in mean, so it is necessary that the regressors

x_t 's are integrated. Indeed, it is not true to represent the non-stationary output y_t by a set of stationary regressors x_t 's, because when x_t 's are non-stationary, it is possible to detect spurious change (Hsu, 2001).

As follows, it is shown that the CUMSUM procedure has weak performance while two game theoretic procedures including best response (Section 2.2) and differential game (Section 4.2) methods have strong performance. To this end, consider the dynamic system (68), with a sensor fault (69) where the Kalman filter (70) is used to estimate the state. Also, assume only that the integrated output y_t^* is available for FDI purpose. The estimation of y_t^* using the Kalman filter estimated output is computed as $\hat{y}_t^* = \int_0^t \hat{y}_s ds$. Two-way FDI methods applied here are the best response function (Section 2.2) and the differential game (Section 4.2).

Here, a CUMSUM method with estimated states, using the Kalman filter, is applied to the scaled series $h_t = \frac{y_t}{x_t}$ (Isermann, 2006). Since, the expectation of h_t is β_t , i.e. $E(h_t) = \beta_t$, thus, the partial sum of the mean corrected series $h_t - \bar{h}$, i.e. $\sum_{i=1}^t (h_i - \bar{h})$, referred to as the CUMSUM method (Isermann, 2006), detects the changes in mean β_t . Indeed, the maximiser of CUMSUM is the change point estimation. The CUMSUM plot with Kalman estimated states is illustrated in Figure 17. Accordingly, the change point estimation is 8 which is far from the actual change point 200. It is seen that the CUMSUM method does not represent the change in β_t at the actual time and instead provides a spurious change point at 8. In previous sections, it was seen that when states are known y_t/x_t is a proxy for β_t , since $E(y_t/x_t) = \beta_t$, and using this stylised fact, based on CUMSUM method, pure and mixed Nash equilibriums are derived. However, when states are unknown, a straightforward suggestion is to use the Kalman estimation of states and consider the CUMSUM of y_t/x_t . By the way, it is seen that this method does not detect the change point. This is why the differential game approach based on Kalman estimation of states and best response method using the LMI solutions are used in

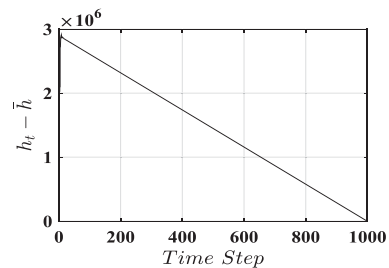


Figure 17. Time Series plot of CUMSUM method, Integrated System.

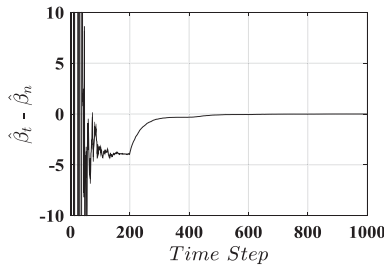


Figure 18. Time Series Plot of $\hat{\beta}_t - \hat{\beta}_n$, Integrated System.

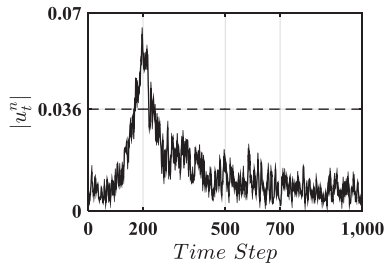


Figure 19. Time Series Plot of $|u_t^n|$, Integrated System.

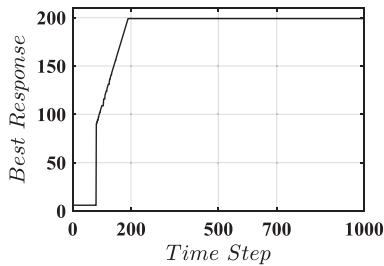


Figure 20. Best response function of both players, Integrated System.

the unknown states case in Section 4. For the differential game approach, the $\hat{\beta}_t$'s $t = 1, 2, \dots, 1000$ are computed. Then, the time series plot of $\hat{\beta}_t - \hat{\beta}_n$ (with $c = -0.4$, see Section 3.3) is shown in Figure 18. It is seen that the actual change point is the first point at which the mentioned plot starts to depart from its initial mean. This plot indicates that the change point estimation is 200. Next, for the best response approach, the time series plot of $|u_t^n|$ result is plotted in Figure 19. Clearly, it crosses the threshold $d = 0.036$ which is the 95% quantile boundary (see Sections 2.3 and 5.1) and takes its maximum at the actual change point. The best response functions of both players are plotted in Figure 20. It is seen again that the Nash equilibrium is the $s = t = 200$.

To study the sensitivity analysis with respect to standard deviation σ_ε , as an important parameter in FDI problems, for $\sigma_\varepsilon = [0.01, 0.1]$, fault estimations \hat{t}_i , $i = \text{br, dg, cu}$ are derived. Notations br, dg and cu stand for best response, differential game, and CUMSUM

methods, respectively. It is seen that $\hat{t}_{\text{br}} = \hat{t}_{\text{dg}} = 200$ which shows that both game theoretic methods detect the change point accurately, and $\hat{t}_{\text{cu}} = 8$ which shows poor performance for the CUMSUM method. However, the two-way game theoretic FDI approaches have good performance, in the integrated system, when the location of the actual change point is too close to the beginning of the data sequence as mentioned in Section 1, Point 9, as well as two-way FDI methods provide two change estimators and by considering the mean of two estimators as the ultimate change estimator, the variance of the ultimate estimator reduces (see Section 1, Point 4).

Here, the reason for good performance of two-way game theoretic FDI methods compared to CUMSUM is explained. Assuming \hat{y}_t and y_t , as well as, y_t^* and \hat{y}_t^* are close to each other, the Kalman filter produces a linear relation between $\int_0^t y_s ds$ and $\int_0^t x_s ds$, with the slope β_t . Thus, using the Kalman outputs of an integrated system, which are $\int_0^t x_s ds$ and $\int_0^t y_s ds$ instead of x_t and y_t , provides the estimation of $\hat{\beta}_t$ very close to the actual β_t when x_t and y_t are used in $\hat{\beta}_t$. Therefore, differential game or best response methods which are based on $\hat{\beta}_t$, perform properly. However, it is not true for the CUMSUM method because it can be simply shown that $E\left(\frac{\int_0^t y_s ds}{\int_0^t x_s ds}\right) = \frac{\int_0^t \beta_s x_s ds}{\int_0^t x_s ds} \neq \beta_t$. Finally, if it can be guaranteed that the available data is integrated, then y_t can be obtained via differentiation of y_t^* . Then x_t can be estimated by the Kalman filter, to which x_t and y_t are fed. Consequently, the mentioned problem is eliminated in the CUMSUM method. However, it is really challenging to ensure that the given data are integrated, in the presence of a fault. Also, differentiation of y_t^* leads to noise amplification problems.

6. Conclusions

In this paper, sensor fault detection was formulated as change point analysis of a linear regression coefficient. The purpose of the paper was application of the game theoretic concepts such as Nash equilibrium and best response functions, to the sensor FDI. Two-way FDI method was introduced at which two players investigate from both sides of the data sequence to detect faults. In the AMOC model, via minimising the bias of estimation of parameters before and after the change point, the two-way FDI game was introduced and it was seen that the Nash equilibrium occurs at the actual change point. Also, the corporative and the competitive game frameworks were introduced in two-way FDI and corresponding Nash equilibriums were derived which occur

at the actual change points. Also, the players' test statistics were given, and their asymptotic null distributions were obtained, to test the existence of the change point, individually by each player. In the known states case, the differential game was presented, and it was confirmed that Nash equilibrium is the true change point. Also, in the unknown states case, Kalman filter and LMI were used to estimate the states. Then via the differential game, accurate results were obtained, similar to the known states case ones. Numerical results showed that the two-way FDI scheme accurately detects the change point, for various fault scenarios. Finally, an integrated servo mechanism was used to evaluate the superiority of proposed scheme compared to the CUMSUM Method.

Acknowledgements

The authors would like to thank the editors and the reviewers for their helpful comments and constructive suggestions, which helped to improve the paper.

Disclosure statement

No potential conflict of interest was reported by the authors.

Notes on contributors

Hamed Habibi received the B.Sc. degree from Khaje Nasir University, Tehran, Iran, in 2010, and the M.Sc. degree from the University of Tehran, Tehran, in 2013, all in mechanical engineering. He is currently pursuing the Ph.D. degree with Curtin University, Perth, Australia. His current research interests include control systems, fault detection, isolation, identification, accommodation, and fault tolerant control with applications on wind turbines.

Ian Howard received the bachelor's and Ph.D. degrees in mechanical engineering from The University of Western Australia in 1984 and 1988, respectively. He was with the Defense Science and Technology Organization for five years. In 1994, he joined Curtin University as a Lecturer in applied mechanics and dynamic systems, where he was promoted to Full Professor in 2016 and continues to supervise research in the dynamic behavior of rotating machinery for fault detection and classification for industry applications.

Reza Habibi has a PhD in Statistics from the Department of Statistics at Shiraz University, Shiraz, Iran. In 2005 he was a visiting researcher in the Department of Mathematics at the University of Ottawa. He has worked on change point analysis in infinite variance observations, Computational Statistics, Stochastic Differential Equations, Game Theory, Data Mining, Financial Mathematics. He has published 67 papers and has written five English books. He was a free researcher in the Department of Statistics at the Central Bank of Iran (CBI). He is currently a lecturer at the Iran Banking Institute of the CBI. He recently graduated in Financial Engineering from Amirkabir University, Tehran, Iran. His research interests include arbitrage pricing, algorithmic trading, applications of heuristic and computational methods in finance, and portfolio management.

ORCID

Hamed Habibi  <http://orcid.org/0000-0002-7393-6235>

References

- Ahmadizadeh, S., Zarei, J., & Karimi, H. R. (2014). Robust unknown input observer design for linear uncertain time delay systems with application to fault detection. *Asian Journal of Control*, 16(4), 1006–1019.
- Alexander, C. (2001). *Market models: A guide to financial data analysis*. Chichester: John Wiley & Sons.
- Aouaouda, S., Chadli, M., Shi, P., & Karimi, H. (2015). Discrete-time H^-/H^∞ sensor fault detection observer design for nonlinear systems with parameter uncertainty. *International Journal of Robust and Nonlinear Control*, 25(3), 339–361.
- Bai, J. (1994). Least squares estimation of a shift in linear processes. *Journal of Time Series Analysis*, 15(5), 453–472.
- Baltazar-Larios, F., & Sørensen, M. (2010). Maximum likelihood estimation for integrated diffusion processes. In C. Chiarella (Ed.), *Contemporary quantitative finance* (pp. 407–423). Berlin, Germany: Springer.
- Başar, T., & Bernhard, P. (2008). *H-infinity optimal control and related minimax design problems: A dynamic game approach*. Cambridge, MA: Birkhäuser Publishing Ltd. Springer Science & Business Media[Q6].
- Billingsley, P. (2013). *Convergence of probability measures*. John Wiley & Sons.
- Blanke, M., Kinnaert, M., Lunze, J., Staroswiecki, M., & Schröder, J. (2006). *Diagnosis and fault-tolerant control*. Springer.
- Ben Brahim, A., Dhahri, S., Ben Hmida, F., & Sellami, A. (2017). Simultaneous actuator and sensor faults reconstruction based on robust sliding mode observer for a class of nonlinear systems. *Asian Journal of Control*, 19(1), 362–371.
- Bresolin, D., & Capiluppi, M. (2013). A game-theoretic approach to fault diagnosis and identification of hybrid systems. *Theoretical Computer Science*, 493, 15–29.
- Bressan, A. (2010). Bifurcation analysis of a non-cooperative differential game with one weak player. *Journal of Differential Equations*, 248(6), 1297–1314.
- Chen, H., & Lu, S. (2013). Fault diagnosis digital method for power transistors in power converters of switched reluctance motors. *IEEE Transactions on Industrial Electronics*, 60(2), 749–763.
- Chung, W. H., & Speyer, J. L. (1998). A game theoretic fault detection filter. *IEEE Transactions on Automatic Control*, 43(2), 143–161.
- Dalei, J., & Mohanty, K. B. (2016). Fault classification in SEIG system using Hilbert-Huang transform and least square support vector machine. *International Journal of Electrical Power & Energy Systems*, 76, 11–22.
- Elhadeif, M., & Grira, S. (2018). Partial syndrome-based system-level fault diagnosis using game theory. *International Journal of Parallel, Emergent and Distributed Systems*, 33(1), 69–86.
- Evans, L. C. (2005). An introduction to mathematical optimal control theory. *Lecture Notes, University of California, Department of Mathematics, Berkeley*.

- Gibbons, R. (1992). *Game theory for applied economists*. Princeton University Press.
- Gu, Y., & Yang, G.-H. (2017). Sensor fault estimation for Lipschitz nonlinear systems in finite-frequency domain. *International Journal of Systems Science*, 48(12), 2622–2632.
- Habibi, H., Howard, I., & Habibi, R. (2017a). Bayesian sensor fault detection in a Markov jump system. *Asian Journal of Control*, 19(4), 1465–1481.
- Habibi, H., Nohooji, H. R., & Howard, I. (2017b). Optimum efficiency control of a wind turbine with unknown desired trajectory and actuator faults. *Journal of Renewable and Sustainable Energy*, 9(6), 063305.
- Habibi, R., Sadooghi-Alvandi, S., & Nematollahi, A. (2005). Change point detection in a general class of distributions. *Communications in Statistics—Theory and Methods*, 34(9–10), 1935–1938.
- Hameed, Z., Hong, Y., Cho, Y., Ahn, S., & Song, C. (2009). Condition monitoring and fault detection of wind turbines and related algorithms: A review. *Renewable & Sustainable Energy Reviews*, 13(1), 1–39.
- Ho, T. K. (1998). The random subspace method for constructing decision forests. *IEEE Transactions on Pattern Analysis and Machine Intelligence*, 20(8), 832–844.
- Hong, L., & Dhupia, J. S. (2014). A time domain approach to diagnose gearbox fault based on measured vibration signals. *Journal of Sound and Vibration*, 333(7), 2164–2180.
- Hsu, C.-C. (2001). Change point estimation in regressions with I (d) variables. *Economics Letters*, 70(2), 147–155.
- Isermann, R. (2006). *Fault-diagnosis systems: An introduction from fault detection to fault tolerance*. Springer Science & Business Media.
- Kander, Z., & Zacks, S. (1966). Test procedures for possible changes in parameters of statistical distributions occurring at unknown time points. *The Annals of Mathematical Statistics*, 1196–1210.
- Li, J., Wang, X., Han, F., & Wei, G. (2017). Fault detection for discrete piecewise linear systems with infinite distributed time-delays. *International Journal of Systems Science*, 1–9.
- Mehranbod, N., Soroush, M., & Panjapornpon, C. (2005). A method of sensor fault detection and identification. *Journal of Process Control*, 15(3), 321–339.
- Murray, E. A., & Speyer, J. L. (2014). A discrete-time game theoretic multiple-fault detection filter. IEEE 53rd Annual Conference on Decision and Control (CDC).
- Mutuel, L. H., & Speyer, J. L. (2000). A discrete-time game-theoretic fault detection filter. American Control Conference.
- Ning, W., Pailden, J., & Gupta, A. (2012). Empirical likelihood ratio test for the epidemic change model. *Journal of Data science*, 10(1), 107–127.
- Petkov, V. (2013). *Continuous mixed strategy equilibria: in static and dynamic tournaments*.
- Pourbabae, B., Meskin, N., & Khorasani, K. (2016). Sensor fault detection, isolation, and identification using multiple-model-based hybrid Kalman filter for gas turbine engines. *IEEE Transactions on Control Systems Technology*, 24(4), 1184–1200.
- Qiu, Y., Feng, Y., Tavner, P., Richardson, P., Erdos, G., & Chen, B. (2012). Wind turbine SCADA alarm analysis for improving reliability. *Wind Energy*, 15(8), 951–966.
- Ren, Y., Ding, D.-W., & Li, Q. (2017). Finite-frequency fault detection for two-dimensional Fornasini–Marchesini dynamical systems. *International Journal of Systems Science*, 48(12), 2610–2621.
- Revuz, D., & Yor, M. (1999). *Continuous martingales and Brownian motion*. Springer-Verlag, Berlin.
- Sen, A., & Srivastava, M. S. (1975). On tests for detecting change in mean. *The Annals of Statistics*, 98–108.
- Song, Y., & Guo, J. (2017). Neuro-adaptive fault-tolerant tracking control of lagrange systems pursuing targets with unknown trajectory. *IEEE Transactions on Industrial Electronics*, 64(5), 3913–3920.
- Wu, L., & Ho, D. W. (2009). Fuzzy filter design for Itô stochastic systems with application to sensor fault detection. *IEEE Transactions on Fuzzy Systems*, 17(1), 233–242.
- Yang, W., Court, R., & Jiang, J. (2013). Wind turbine condition monitoring by the approach of SCADA data analysis. *Renewable Energy*, 53, 365–376.
- Yunlong, Z., & Peng, Z. (2012). Vibration fault diagnosis method of centrifugal pump based on emd complexity feature and least square support vector machine. *Energy Procedia*, 17(1), 939–945.
- Zarei, J., & Shokri, E. (2014). Robust sensor fault detection based on nonlinear unknown input observer. *Measurement*, 48, 355–367.
- Zhang, J., Swain, A. K., & Nguang, S. K. (2015). Robust sliding mode observer based fault estimation for certain class of uncertain nonlinear systems. *Asian Journal of Control*, 17(4), 1296–1309.